Geomorphology 240 (2015) 102–120

Contents lists available at ScienceDirect

Geomorphology

journal homepage: www.elsevier.com/locate/geomorph

River meandering on Earth and Mars: A comparative study of Aeolis Dorsa meanders, Mars and possible terrestrial analogs of the Usuktuk River, AK, and the Quinn River, NV

Yo Matsubara [a,*], Alan D. Howard [b], Devon M. Burr [c], Rebecca M.E. Williams [d], William E. Dietrich [e], Jeffery M. Moore [f]

[a] Center for Earth and Planetary Studies, National Air and Space Museum, Smithsonian Institution, Independence Ave., 6th St. SW, MRC 315, PO Box 37012, Washington, DC 20013-7012, United States
[b] Department of Environmental Sciences, University of Virginia, P.O. Box 400123, Charlottesville, VA 22904-4123, United States
[c] Department of Earth and Planetary Sciences, University of Tennessee, 1412 Circle Dr., Knoxville, TN 37996-1410, United States
[d] Planetary Science Institute, 1700 East Fort Lowell, Suite 106, Tucson, AZ 85719-2395, United States
[e] Department of Earth and Planetary Sciences, University of California, Berkeley, 307 McCone Hall, Berkeley, CA 94720-4767, United States
[f] NASA Ames Research Center, MS 245-3, Moffett Field, CA 94035-1000, United States

ARTICLE INFO

Article history:
Received 2 May 2014
Received in revised form 11 August 2014
Accepted 28 August 2014
Available online 16 December 2014

Keywords:
Meandering rivers
Terrestrial analog
Aeolis Dorsa
Mud-dominated
Permafrost controlled

ABSTRACT

The paleo-meanders in the Aeolis Dorsa (AD) region show that meandering channels can develop in the absence of vegetation. Three possible mechanisms other than vegetation could contribute to the bank cohesion required to promote meandering: permafrost, abundant mud, and chemical cementation. Banks at the meandering Quinn River show little vegetation cover. Almost all sediment samples collected from the Quinn River deposits contain at least 41% mud (silt/clay), which is much higher than for most meandering streams. Ion chromatography (IC) analysis and scanning electron microscope (SEM) images showed presence of salts in river waters and sediments which may induce fine sediment to flocculate and be deposited. We find that bank cohesion promoting meandering can be provided by silt/clay, the deposition of which may be induced by dissolved salts. The sinuous Usuktuk River in the continuous permafrost region near Barrow, Alaska exhibited no exposed permafrost on stream banks. Instead vegetation seemed to be the dominant control of bank erosion. We have not found evidence for ice control of bank cohesion in this or other terrestrial rivers of similar size and in meandering pattern to the Martian AD meanders. We conclude that bank cohesion in the AD meanders was probably provided by deposition of fine suspended sediment that was flocculated by dissolved salts.

1. Introduction

Highly sinuous paleo alluvial channels with attendant floodplains and cutoffs have been found in high resolution imaging of Mars (Malin and Edgett, 2003; Moore et al., 2003; Burr et al., 2009, 2010; Williams et al., 2013). These features present a dilemma in accounting for this meandering, because most terrestrial meandering channels are associated with an appreciable vegetation cover, which has been postulated as being important in producing meandering as opposed to braiding morphology. The existence of these prominent meanders on presumably vegetationless Mars requires explanation. In this paper we discuss the setting and properties of the Martian meandering paleochannels, review the literature on factors producing cohesive stream banks permitting meandering versus braided channels, and explore two possible terrestrial analog sites.

1.1. Aeolis Dorsa (AD) meanders, Mars

Several Martian valley systems have undergone extensive aeolian deflation of fine-grained deposits, leaving channels in inverted relief (Williams and Edgett, 2005; Pain et al., 2007; Williams, 2007; Mangold et al., 2008; Newsom et al., 2010). Most of these are fragmentary or exhibit low sinuosity, but an extensive set of inverted sinuous channels is exposed in the Aeolis Dorsa region, centered at about 5°S and 150°E (Burr et al., 2009, 2010; Williams et al., 2009, 2013) (Fig. 1). In some areas sinuous ridges with multiple bends can be traced in the Mars Reconnaissance Orbiter (MRO) Context Camera (CTX) images (6 m/pixel) (Malin et al., 2007) with apparent cutoffs and parallel lineations that resemble scroll bar deposits in terrestrial meandering channels (Fig. 2a, b).

The AD meanders are developed in the basal member of the Medusae Fossae Formation (MFF), which is likely deposit of volcanoclastic origin (Bradley et al., 2002; Hynek et al., 2003; Carter, 2009; Mandt et al., 2009). The extensive aeolian erosion of this formation into yardangs (Figs. 1, 2) indicates a friable nature (Ward, 1979; Scott and Tanaka, 1982; Bradley et al., 2002; Hynek et al., 2003; Mandt et al., 2008, 2009;

* Corresponding author. Tel.: +1 202 633 2479.
E-mail address: matsubaray@si.edu (Y. Matsubara).

http://dx.doi.org/10.1016/j.geomorph.2014.08.031
0169-555X/

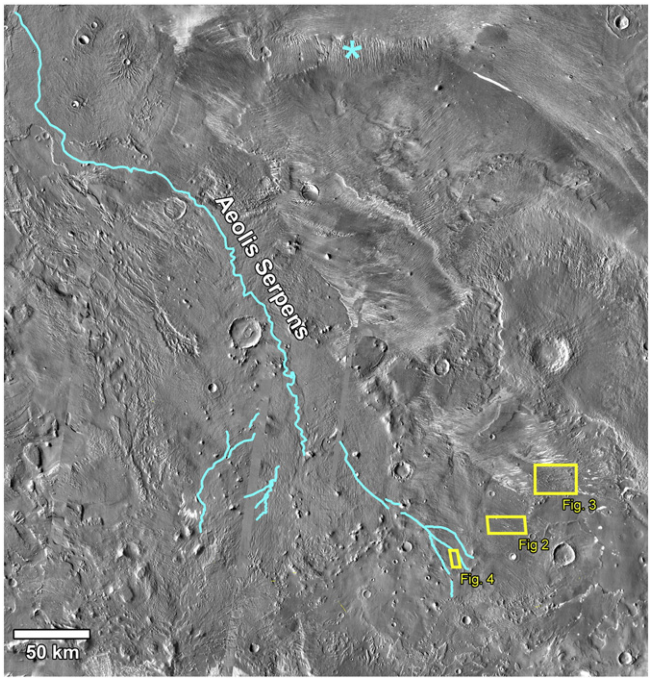

Fig. 1. Map of major inverted channels and figure locations in the Aeolis Dorsa region, Mars. Approximate image bounds 148.65–155.74°E, 0.27°N–7.17°S. Image base 100 m/pixel THEMIS daytime IR with blanks filled by MDIM 2.1 images. Blue lines are major inverted channels. Yellow boxes with numbers show locations of numbered figures. Examples of large yardangs are shown by an asterisk (*).

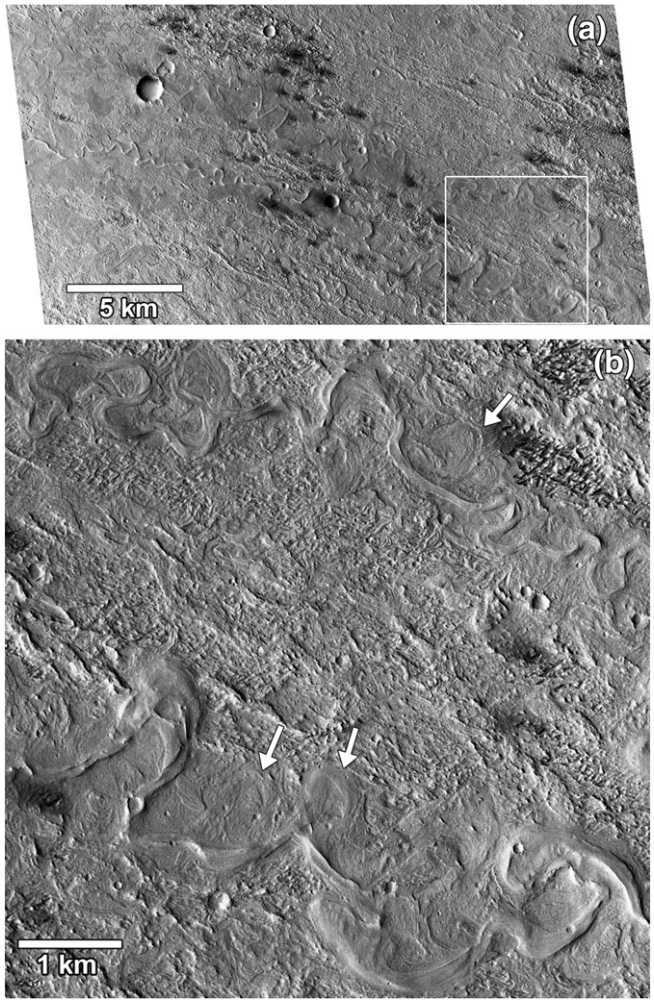

Fig. 2. Meandering channels in the Aeolis Dorsa region. Image centered at 154.205°E, 5.535°S. (a) Several parallel sets of inverted meandering channels. (b) Detail of two inverted meandering channels and associated floodplain deposits. Arrows point to representative cutoff loops. Fluvial deposits are relatively smooth-surfaced. Rough terrain, such as near (b) and the scale bar is fine-grained deposits of the Medusa Fossae Formation that is wind-eroded into short yardangs. Faint traces of smaller channels also occur between the two main channel systems. Location of image shown by box in (a). Image is part of CTX image P05_002589_1750. See Fig. 1 for location.

Carter, 2009; Zimbelman and Griffin, 2010). Age estimates of the MFF based on crater counts place deposition in the Amazonian (Tanaka, 1986; Werner, 2006), but the extensive deflation of the deposit likely results in a misleadingly young crater-based age, and more recent dating indicates a Hesperian age (Burr et al., 2009; Kerber and Head, 2010; Zimbelman and Scheidt, 2012). Crater-count dating by Kite et al. (2014) suggests a Hesperian to Late Noachian age for the fluvial activity.

Many of the exposures of the AD meandering channels are fragmentary or strongly eroded (e.g., Fig. 3). The discussion here emphasizes a ~15 km exposure of paleomeanders that exhibits strong sinuosity (~1.5–2.3), evidence of historical evolution of meander bends through channel migration, evidence of cutoffs and avulsions, and is imaged at high resolution (25 cm/pixel) in stereo (Fig. 4a). Less well-exposed sinuous meander belts occur to the southwest (Fig. 4a), outlined in violet in Fig. 4b. These meanders may be smaller or possibly older and are not as well exposed by deflation. Younger, and stratigraphically higher meandering channels occur within the mapped area (light brown). The channel patterns are less well exposed on these younger meander belts, at least in part from greater aeolian stripping. Note that the location of the valleys shifted between the older and lower meanders and the younger valley deposits, possibly because of a MFF depositional event burying the older valleys.

Fig. 5 shows a short section of one meandering channel exhibiting highly sinuous loops. The interior of the large bends shows a series of sub-parallel benches that record earlier positions of the channel and the migration of the meander bends (Fig. 6). In recording the path of meander migration these resemble point bars on terrestrial river floodplains (e.g., Fig. 7). It is likely that these interior benches are channel floor deposits rather than point or scroll bars, however, because the benches topographically become higher upon progressing from the interior to the exterior of the bends (i.e., from earlier- to later-deposition), as revealed in stereo anaglyphs (e.g., from 1 to 2 in Fig. 5). By contrast, point bars generally increase in height towards the interior of bends due to continued deposition. The point bars, and scrolls, if they were present, have presumably been stripped by aeolian erosion. This pattern implies that the channel was aggrading during meander evolution.

The stereo anaglyphs were utilized to interpret the evolution of two channel systems converging to the northwest. Three types of channel cutoffs — neck cutoffs, chute cutoff, and large avulsions — occurred during the time period recorded by the green, blue, and black stages in channel evolution in Fig. 4b. Some meander loops grew large enough to trigger neck cutoffs (arrow in Fig. 5a). A probable chute cutoff is illustrated in Fig. 8, with the original loop extent shown by the black arrow and the cutoff by the white arrow. Many short chute cutoffs across bend apices may not have left a record, because meanders often reoccupy the abandoned loops during subsequent migration. Several cutoffs are transitional, involving short chute cutoffs of a high-amplitude bend at the location where a neck cutoff would eventually have occurred (e.g., red dots in Fig. 4b). Finally, large avulsions occurred across several meander loops in the northern mapped channel (Fig. 9). The final channel courses (black in Fig. 4b) appear to be less sinuous (~1.5) than earlier channels (up to ~2.3), particularly after the avulsion event in the northern channel. These cutoffs and avulsions were probably facilitated by progressive aggradation of the fluvial system in this location, which also aids recognition of the temporal sequence.

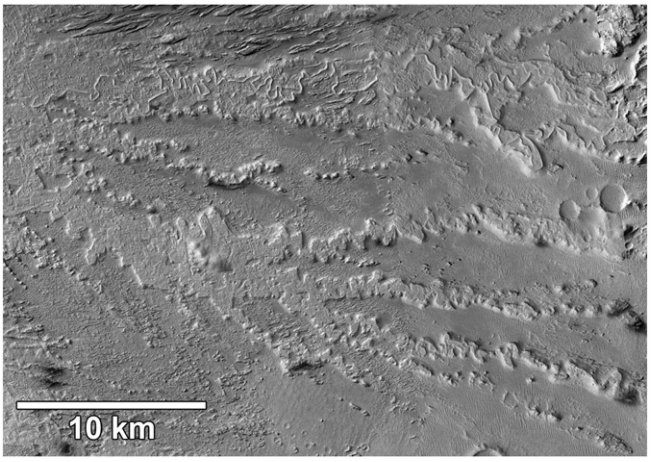

Fig. 3. Converging inverted valleys in the Aeolis Dorsa region. Flat-topped ridges are interpreted to be paleo floodplain deposits resulting from lateral migration of meandering streams with abandoned cutoff loops. Composite landform near top of image features sinuous inverted channel superimposed on plateau of inverted floodplain deposits. This channel is interpreted to result from aggradation of the channel near the termination of fluvial flows. Aeolian deflation has inverted the valley floors through preferential erosion of the fine-grained Medusa Fossae Formation whose higher stratigraphic layers which, at the time of fluvial activity, would have formed divides between the valley networks. Image is CTX image mosaic centered at 154.74°E, 5.02°S. See Fig. 1 for location. Prominent yardangs are present at the top left of the image.

The sedimentary characteristics of the AD meanders are difficult to infer without ground truth. Full resolution images of the meanders (e.g., Figs. 7 and 8) reveal no obvious meter-scale boulders. This lack of boulders is not surprising given the probable fine-grained nature of the MFF deposits. A platy surface structure suggestive of cohesive strength is evident in some images of meander deposits (Fig. 7). The deposits also can sustain expression of fractures as well as the imprint of small craters. On the other hand, exposed channel deposits do not weather into multi-meter angular blocks as are evident on the sides of some yardangs sculpted into the MFF (Zimbelman and Griffin, 2010). The channel deposits are also not eroded into yardangs like the MFF, and they are able to stand in positive relief as MFF deposits are deflated. Based upon these characteristics, the exposed channel deposits are likely to be slightly-cemented fine to medium textured gravel (Burr et al., 2010; Williams et al., 2013). This grain size is also inferred from the moderately high thermal inertia of the channel deposits (Burr et al., 2010), although the high thermal inertia could result from finer, but cemented bed sediment.

Because of the inferred fine-grained composition of the MFF, it is likely that the meandering streams carried a large concentration of suspended load. High concentrations of suspended load are likely under the reduced gravity of Mars (Komar, 1979, 1980b). The suspended load presumably formed cohesive point bar and overbank deposits that constrained the channel width sufficiently to promote meandering rather than a braided channel pattern. Yet, only channel deposits appear to be exposed in the inverted meanders, implying

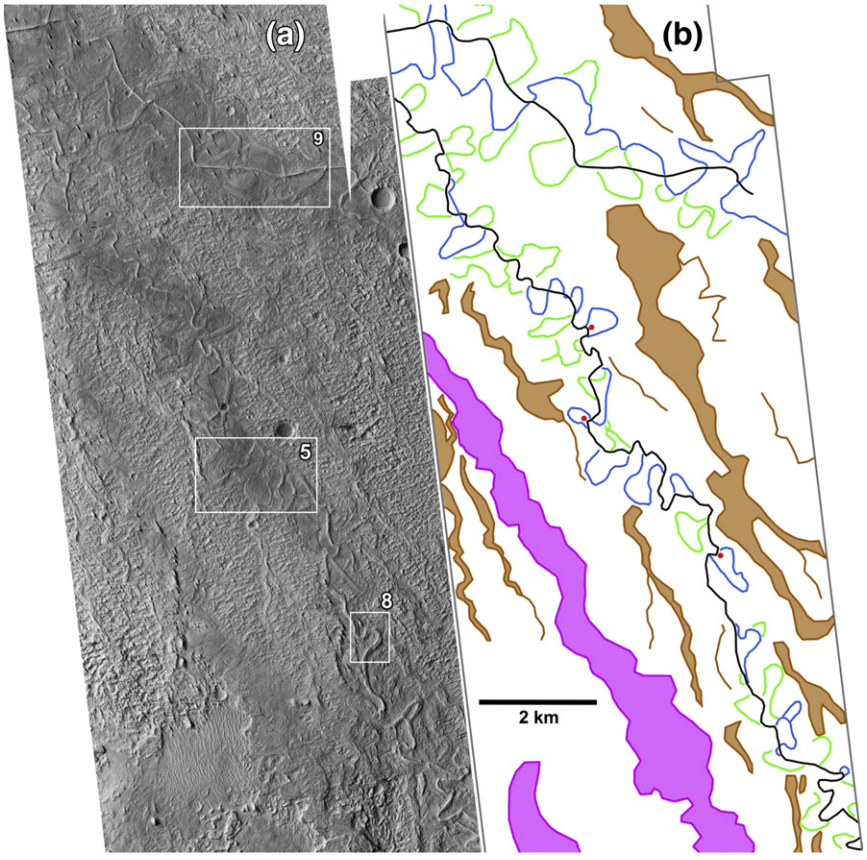

Fig. 4. Image mosaic of HiRISE images showing well-expressed meandering channel features. See Fig. 1 for general location. (a) Mosaic composed of parts of rectified HiRISE images PSP_006683_1740 and PSP_010322_1740 centered at 153.63°E, 5.96°S. Boxes show locations of Figs. 5, 8, and 9. (b) Interpretation of channel features. Features of two channels are shown in detail. Black lines show interpreted final path of the channels. Blue lines are channel sections abandoned shortly before flow cessation, and green lines are older abandoned meander loops. Channel complex is inferred to have undergone progressive aggradation during meander evolution. Violet area encloses meandering channel complexes not mapped in detail. Brown lines and enclosures show younger, higher meander channel complexes in advanced state of erosion. Red dots indicate chute cutoffs across necks of high amplitude meanders.

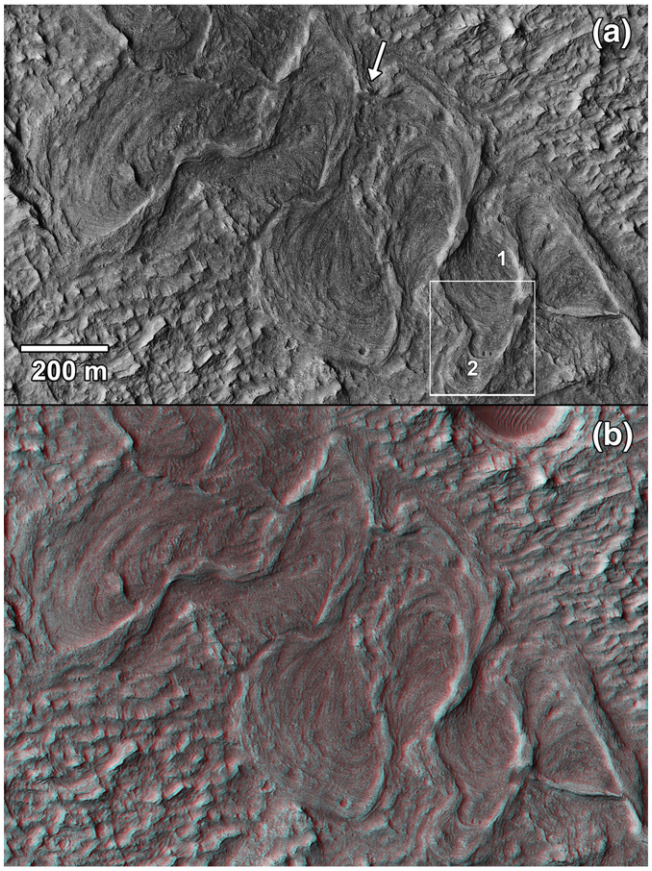

Fig. 5. Sequence of tight meander bends in area mapped in Fig. 4. (a) HiRISE image outtake showing highly sinuous meanders and curved interior benches marking former channel positions and the course of meander migration. A late-stage neck cutoff is inferred to have occurred near the white arrow. Location of Fig. 7 shown in white box. Rough ridges near "200 m" and "(a)" are yardangs excavated into the Medusa Fossae Formation. (b) Part of a stereo anaglyph image from HiRISE images PSP_010322_1740 and PSP_006683_1740 showing progressive aggradation of the channel during the enlargement of meander bends. Note that this anaglyph is not rectified.

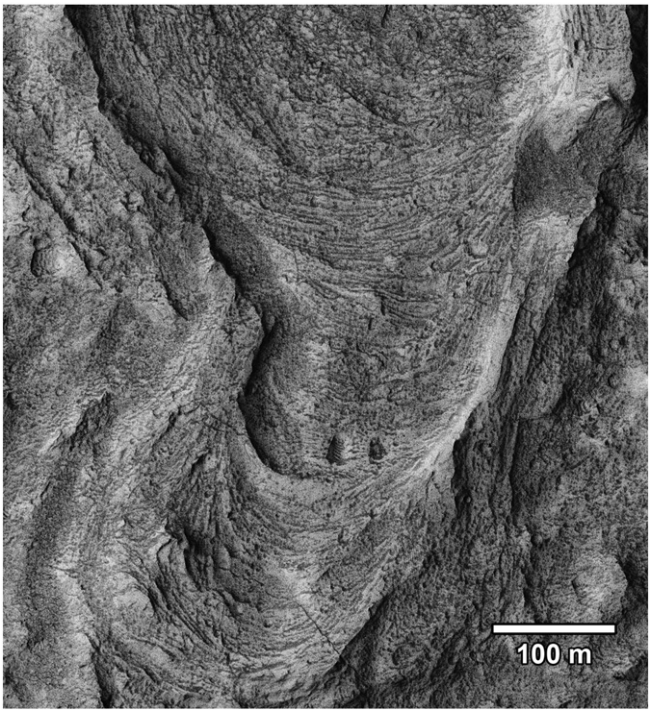

Fig. 6. Full resolution HiRISE image showing pattern of meander migration. Interior benches are inferred to be earlier channel bed deposits. Note the absence of meter-scale boulders, the platy character of the interior deposits, and the preservation of small cracks and impact craters. Outtake from HiRISE image PSP_006683_1740. Channel is inferred to have aggraded as the meander loop enlarged. See Fig. 5 for location.

that the overbank deposits must be readily stripped by aeolian erosion and are more easily eroded than the MFF deposits. The composition of overbank deposits is, thus, uncertain. Exposures of clay-rich fine fluvial overbank sediment can be readily eroded by saltating sand (Morgan et al., 2014), even though they are strongly cohesive when dry. Although no clays have been detected by CRISM multispectral observations covering the AD meandering channels, results from the Mars Science Laboratory (MSL) rover show that a high percentage of clays in sediment may not be detected by the CRISM instrument (Bristow et al., 2013).

Channel-forming discharges have been estimated for the AD channels based upon channel widths and meander wavelengths as scaled for the lower Martian gravity (Burr et al., 2010; Williams et al., 2013). Burr et al. (2010) estimated discharges for 16 channel sections ranging in width from 48 to 106 m and wavelengths from 700 to 2500 m, yielding flood discharges primarily in the range of 200–1000 m^3/s. Williams et al. (2013) applied similar techniques to the larger Aeolis Serpens channel (Fig. 1), measuring widths from 100 to 500 m and wavelength of ~5500 m, yielding flood discharges between 1700 and 4000 m^3/s. The channels mapped in Fig. 4b are smaller. The central northwest–southeast trending channel has an average width of about 51 m and a wavelength averaging 409 m. The east–west channel at the north end of Fig. 4 has a width averaging 91 m and a wavelength of 835 m. The unmapped meandering channels within the area enclosed by violet lines average about 31 m in width and 265 m in wavelength. Formative discharges would be correspondingly lower. The wavelength to width ratio for these channels is in the range of 8–9, towards the lower end of the range of 8–16 observed in terrestrial meandering channels (Williams, 1986, 1988). Estimates of channel width from these largely uneroded channels may be biased towards high values because of channel migration. On the other hand, the more eroded channels, such as the avulsed channel in Fig. 9, yield wavelength to width ratios higher than the terrestrial range (Burr et al., 2010).

Unconfined meandering channels, such as those in AD, imply that migration occurred freely cross a floodplain. The evolution up to cutoff of highly sinuous, single-thread channels in the absence of a biotic binding mechanism for the floodplain sediment presents a challenge: what maintains channel coherence?

1.2. Conditions for meandering and floodplain formation

The planform characteristics of streams (channel patterns) reflect their formative hydrologic and sedimentary environment. The earliest systematic investigation of channel patterns identified three major types, straight, meandering, and braided (multiple flowpaths at low flow) and suggested that thresholds occur between meandering to braided as valley gradient and dominant channel discharges increase (Leopold and Wolman, 1957, 1960). Subsequently a fourth major pattern, anastomosing (anabranching) was identified characterized by multiple channels separated by vegetated floodplain surfaces (Knighton and Nanson, 1993; Nanson and Knighton, 1996; Makaske, 2001).

The influences of flow intensity, valley gradient, size and quantity of bedload and suspended load, as well as vegetation on channel pattern are primarily related to the effects on the flow stresses and bank erodibility. These influences are largely expressed through the aspect ratio ($\gamma = W/H$) and this ratio has been used as a criterion for characterizing the threshold between meandering and braided patterns (Engelund and Skovgaard, 1973; Fredsoe, 1978; Fukuoka, 1989; Howard, 1996). If channel banks are largely unvegetated and composed of cohesionless

Fig. 7. Scroll bars along the Quinn River, Nevada, USA. (a) Prominent scroll bars indicate by an asterisk (*). (b) Lidar topography of the same location. Center of image at 41.217°N, 118.741°W.

sediment, channels will be wide, γ will be high (>50), and a braided pattern will tend to develop because of channel bed instabilities related to development of multiple alternate bars (Engelund and Skovgaard, 1973; Parker, 1976; Fredsoe, 1978; Fukuoka, 1989; Seminara and Tubino, 1989; Howard, 1996; Dade, 2000; Crosato and Mosselman, 2009). On the other hand, if banks are cohesive (e.g. clay rich, cemented, or densely vegetated) meandering channels will form (usually $10 < \gamma < 50$). Channel width and the degree of channel sinuosity have been found to be proportional to the percentage of clay in channel bed and banks (Schumm, 1960, 1963a, 1968a; Ferguson, 1987). A rich literature documents the effects of vegetation on channel morphology, with channels being narrow and deeper (lower γ) with densely vegetated banks (e.g., Graf (1978), Andrews (1984), Hickin (1984), Hey and Thorne (1986), McKenney et al. (1995), Friedman et al. (1996), Huang and Nanson (1997), Huang and Nanson (1998), Moody et al. (1999), Millar (2000), Van De Wiel and Darby (2004), Van de Wiel and Darby (2007)). Differences in the types of vegetation (e.g. forested versus meadow) are often associated with differences in channel width (e.g., Zimmerman et al. (1967), Charlton et al. (1978), Murgatroyd and Ternan (1983), Davies-Colley (1997), Trimble (1997), Hession et al. (2003), Trimble (2004), Allmendinger et al. (2005)). Similarly, meander

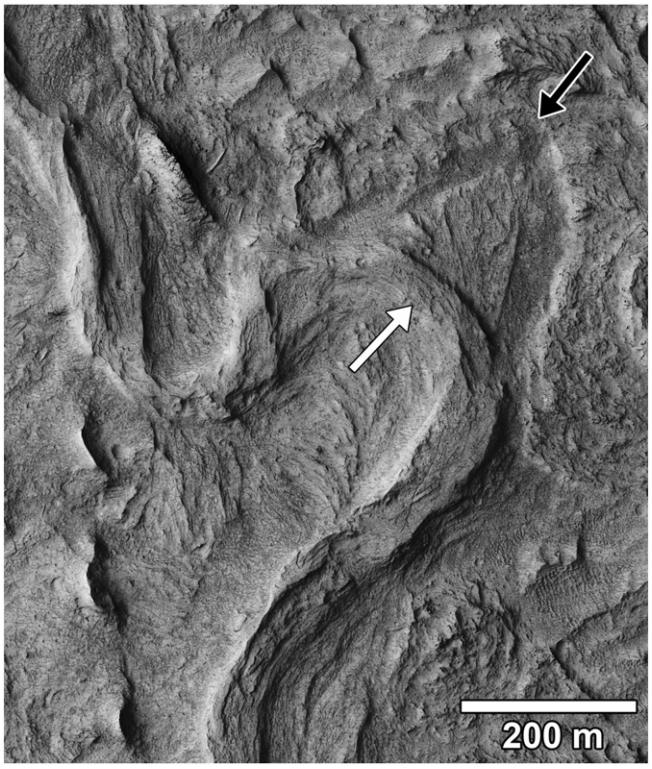

Fig. 8. Inferred chute cutoff. Black arrow points to apex of former abandoned meander loop, and white arrow points to chute cutoff. Outtake from HiRISE image PSP_006683_1740. See Fig. 4 for location.

migration tends to be slower when banks are more densely vegetated (Odgaard, 1987; Pizzuto and Meckelnburg, 1989; Micheli et al., 2004; Allmendinger et al., 2005).

Parker et al. (2011) summarize and model the vital role of bank cohesion in facilitating meandering versus braiding. In an alluvial channel if the outer banks are non-cohesive, then erosion will rapidly outpace deposition and the channel will widen to the point that chute cutoffs would form, limiting development of sinuosity (e.g., Frederici and Seminara (2003)) and promoting a braided pattern. Similarly, deposition on the inner-bank must keep pace with outer-bank erosion or the channel will likewise widen and develop a braided pattern. Sediment is initially deposited loosely on the inner bank. If it is not stabilized, fluid stresses will re-entrain the sediment. Cohesion of inner- and outer-banks is most commonly obtained through vegetation, cohesive sediment, or bedrock (e.g., Murray and Paola (1994)). In most terrestrial meandering streams vegetation plays a dominant role in providing bank cohesion.

Fig. 9. Abandonment of meander loops through avulsion. Relatively straight strongly inverted channel is assumed to have resulted from avulsion of lower, more sinuous channels. Outtake from HiRISE image PSP_006683_1740. See Fig. 4 for location.

The importance of bank cohesion in producing meandering channel patterns is illustrated by the difficulty in producing highly sinuous channels in a laboratory setting. Almost all experimental, self-formed meandering channels with alluvial banks have sinuosity less than 1.5 as a result of the difficulty in obtaining low width/depth ratios (e.g., Friedkin (1945), Schumm and Khan (1971), Schumm et al. (1987)). This occurs largely because of the difficulty in a scale model to duplicate the formation of cohesive banks by overbank sedimentation of clays or development of vegetation. Some success has been achieved in creating slightly higher sinuosity by eroding channels into cohesive sediment (Smith, 1998), but the higher sinuosity channel pattern is generally ephemeral because bank erosion eventually erodes the cohesive sediment and a low-sinuosity or braided channel pattern emerges (Federici and Paola, 2003), unless cohesive silt is introduced as part of the sediment load (Kleinhans, 2005). Introduction of vegetation (e.g. sprouts) on a scale model floodplain also permits development of sinuous channels when accompanied by suspended fine sediment (Braudrick et al., 2009), and vegetation reduces the degree of braiding in experimental channels (Gran and Paola, 2001; Tal et al., 2004). van Dijk et al. (2012) develop moderate sinuosity experimental channels by incorporating fine silt into the sediment feed coupled with a laterally oscillating flow and sediment inlet. At best, however, experimental meanders created to date experience chute cutoffs but do not create sufficient sinuosity to develop neck cutoffs.

Two important conclusions emerge from studies of natural and laboratory meandering streams. One is that the channel requires a cohesive floodplain (Seminara, 2006) or else new channels will form until they develop into a braided channel (Tal et al., 2004). The second conclusion is that floodplain cohesion must redevelop or be maintained within newly-deposited point bar and overbank sediment on the timescale of meander migration in order that the meandering pattern persists. Otherwise a sinuous meandering pattern might initially form but be quickly replaced by braiding or low-sinuosity meandering.

The appearance of meandering channels in the geologic record coincides with introduction of plants on land during the Devonian period (Schumm, 1968b; Cotter, 1978; Long, 1978; Eriksson et al., 1998; Tirsgaard and Oxnevad, 1998; Davies and Gibling, 2010a,b) and distinctive sandy floodplain assemblages (Fralick and Zaniewski, 2012), in part because of lack of bank cohesion and in part because of fewer fines produced by weathering. This suggests that vegetation is essential for channels to meander rather than braid.

The sinuous meanders in the Aeolis Dorsa (AD) region on Mars comprise a compelling argument, however, that meandering channels can develop in the absence of vegetation in certain geomorphic settings. Because of the common association of terrestrial meanders with vegetation, other mechanisms providing bank stability have been understudied. Here, we assess the role of lower Martian gravity, clays, chemical cementation, and permafrost on development of meandering channels with an emphasis on finding mechanisms other than vegetation for forming meandering channels given the unlikelihood of the past presence of vegetation on Mars. We first consider the possibility that the lower Martian gravity (~38% of gravity on Earth) may facilitate meandering. In the terrestrial context of highly sinuous channels in the continuous permafrost region of the North Slope of Alaska we consider the possibility that ice within river bank sediment might provide sufficient cohesion to promote active meandering, as suggested by Moore et al. (2003) and Dietrich and Perron (2006). We then describe the meandering Quinn River in Nevada, which exhibits highly sinuous meandering in clay-rich sediments with appreciable solute involvement. These potential terrestrial analogs are similar in size and meander properties to the AD channels (Table 1).

1.3. Effect of lower Martian gravity on meandering

Here we address the question — does the lower gravity of Mars influence sedimentary processes in a manner that makes it easier obtain a meandering planform? A variety of studies have used scaling relationships to assess formative sedimentary and hydrologic conditions for Martian channels (e.g. Komar (1979, 1980a,b), Komatsu and Baker (1997), Moore et al. (2003), Burr et al. (2004), Wilson et al. (2004), Irwin et al. (2005a,b), Kleinhans (2005), Howard et al. (2007, 2008), Irwin et al. (2008), Burr (2011)), but only the speculative abstracts by Komar (1980a) and Ori et al. (2013) have addressed channel pattern. Empirical studies of the threshold between meandering and braiding understandably do not include the potential effects of gravity. Most theoretical studies of the threshold likewise do not explicitly contain gravity scaling or they include empirical relationships as part of the derivation, an issue noted by Kleinhans (2010). Two semi-theoretical studies of the hydraulic geometry of sand-bed (Wilkerson and Parker, 2011) and gravel-bed (Parker et al., 2007) rivers do explicitly include gravity scaling. The channels forming the calibration database for this study are, however, affected to varying degrees by vegetation on the banks and point bars.

The effect of gravity on the threshold between meandering and braided channel patterns can be evaluated through considering the relative degrees of bank cohesion required to maintaining a meandering pattern on Mars versus Earth. Parker (1976) developed a relationship for the threshold of braiding, ε:

$$\varepsilon = SW(\pi HF)^{-1} \tag{1}$$

where W, H, and S are the width, mean depth and gradient of the channel width, and F is the Froude Number, $F = U(gH)^{-1/2}$, where g is gravity and U is mean velocity. Braiding is indicated to occur for values of $\varepsilon > 1$. The threshold defines when multiple bars would form across an alluvial channel bed. Both experiments (Fugita, 1989) and simulation modeling (Murray and Paola, 1994) suggest that channels with multiple bars develop instabilities resulting in a braided pattern.

We assume that the cross-sectional shape of the channel is determined by a critical shear stress, τ_c, across the bed and banks that balances long-term erosion and deposition. Assuming discharge $Q = HWU$, $\tau = \rho gHS$, and an equivalent friction factor, f, on the two planets, $f = 8gHSU^{-2}$, and the meandering–braiding transition from Eq. (1), then:

$$\varepsilon = (\rho S)^{5/2} Q g^2 f \tau_c^{-5/2} (8\pi)^{-1}. \tag{2}$$

Table 1
Characteristics of Martian and terrestrial meandering streams.

	Aeolis Dorsa, Mars	Quinn River, Nevada	Usuktuk River, Alaska
Channel width (m)	30–106	20	100
Meander wavelength (m)	400–2000	300	1780
Bed sediment	Sand or fine gravel[a]	Mud	Sand
Channel gradient	Unknown	0.00015	0.0002

[a] Sediment size inferred from analysis of orbital data and deposit morphology.

To evaluate the relative critical shear stresses for an equivalent channel pattern on Earth (E) and Mars (M) we compare channels with equivalent gradients and discharges. This implies:

$$\frac{\tau_{cM}}{\tau_{cE}} = \left(\frac{g_M}{g_E}\right)^{4/5} = 0.46. \quad (3)$$

This suggests that a meandering pattern might occur on Mars for considerably smaller values of bank cohesion than on Earth. Theoretical extrapolation from Earth to Mars is always uncertain, however, without specific information on channel geometry, flow depths, flow resistance, and sediment characteristics (bed and banks) that pertained during the formative flows (Kleinhans, 2005).

2. Possible terrestrial analogs

2.1. Barrow, Alaska

The circumpolar Arctic hosts large numbers of strongly meandering rivers in the zones of continuous and discontinuous permafrost. They are prevalent up to latitudes of more than 72°N in Alaska and Siberia in sediment-mantled regions not covered by late Pleistocene glaciers. Exposures of ice, either as ice wedges or massive bedded ice are common on eroding banks of larger rivers (e.g. Walker and Arnborg (1966), Walker et al. (1987), Costard et al. (2003), Walker and Hudson (2003), Rowland et al. (2009)) and erosion of river banks is often attributed to be dominated by thermo-erosional niching (Walker and Arnborg, 1966; Lewellen, 1972; Scott, 1978; Walker et al., 1987; Costard et al., 2003; Gautier et al., 2003; Walker and Hudson, 2003). This suggests that cohesion introduced by interstitial or massive ice in river banks limits rates of bank erosion and might provide the bank stability necessary to favor meandering over braided stream patterns. The portions of the Arctic supporting meandering stream channels also support taiga or tundra vegetation, which may also provide cohesion and promote a meandering channel pattern (Vandenberghe, 2001, 2002; Huisink et al., 2002).

If cohesion introduced by frozen stream banks is a major factor controlling stream morphology, the Arctic meandering streams may be a close analog to the Martian meanders. If, however, vegetation dominates in permitting a meandering pattern then a close analog is unlikely. To address this, we investigate meandering rivers in the vicinity of Barrow, Alaska that exhibit similar planform morphology to the Martian AD meanders.

In large arctic rivers and deltas lateral erosion generally occurs by notching of the lower parts of river banks and undermining and collapse or slumping of the more cohesive, frozen, and generally vegetated upper portions of the bank (Lewellen, 1972; Scott, 1978; Walker et al., 1987; Walker and Hudson, 2003; Walker and Jorgenson, 2011). Seasonal depth of thaw can reach 50 cm in coarse sediment, but can be only a few centimeters in cohesive sediment (Scott, 1978). Thermo-mechanical erosion can be limited either by depths of thaw or by the ability of streams to erode and transport thawed sediment. Scott (1978) suggests rates of bank erosion are commonly less than seasonal depth of thaw. On the other hand, in large rivers thermo-mechanical notching and attendant bank retreat can exceed 3–5 m, with extremes exceeding 8 m for an individual event (Walker et al., 1987; Walker and Hudson, 2003; Walker and Jorgenson, 2011). But average rates of bank erosion in bends of large rivers is more typically 0.9 m per year and less for cohesive banks, with local maximum rates several times higher (Walker et al., 1987; Gautier et al., 2003; Walker and Jorgenson, 2011). Cases of very rapid bank erosion probably have a strong component of mechanical entrainment (Gautier et al., 2003). In summary, rates of bank erosion can be limited either by seasonal depths of thaw (as accelerated by contact with river flows) or by the ability of the flow to detach and transport the thawed sediment.

The strongly sinuous meandering of rivers heading on the Arctic Coastal Plain display a strong visual similarity to the AD meanders. We have investigated meandering channels in the region south of Barrow, Alaska in terms of the analog potential (Fig. 10). The two related questions to be addressed are as follows: 1) Is a meandering pattern maintained as a result of cohesion introduced by frozen banks? And 2) does vegetation have a strong effect on evolution of arctic channel morphology?

The Coastal Plain is mantled by a thin mantle (a few tens of meters) of Quaternary sediment collectively termed the Gubik Formation (Black, 1964; Jorgenson et al., 2011) overlying Cenozioc and earlier deformed sedimentary rocks. The fluvial network is incised into this mantle. The Gubik Formation has several distinct facies, including marine sands and silts deposited during transgressive interglacial highstands and (largely stabilized) sand dunes and loess (Williams et al., 1977, 1978; Williams, 1983; Jorgenson et al., 2011). In the Barrow area the coastal region is underlain by diverse facies largely composed of marine sands and silts, with minor gravel. Black (1964) designates this as the Barrow Unit. South of Barrow, the Gubik Formation is dominantly sandy with minor silt, termed by Black as the Meade River Unit. The Meade River unit has been interpreted as a paleo sand sea (Carter, 1981), and transitions to loess along its southern margin (Jorgenson et al., 2011). The boundary between these two units lies approximately along the SW–NE trending portion of the Meade River (Fig. 10).

Although the Barrow and Meade River units of the Gubik Formation feature strongly meandering rivers, we limit our study to meandering channels in the Meade River unit and focus on a prominent tributary, the Usuktuk River. The finer Barrow unit typically has a thick peat horizon and dense vegetation, which presumably limits its analogy to Mars. In addition, most of the smaller rivers in this unit appear to be geomorphically largely inactive with poorly-developed point bars, beaded drainage in smaller channels, and patterned ground (ice wedges) extending deep into the interior of meander bends. Channels developed in the sand dunes and loess of the Meade River unit have well-developed point bars, numerous cutoffs and oxbow lakes, and a less dense vegetation cover.

We have primarily investigated the sinuous lower portion of the Usuktuk River, a tributary to the Meade River (Fig. 11). We employed DOQ (Digital Ortho Quadrangles), historical aerial photography downloaded from the EarthExplorer (http://earthexplorer.usgs.gov), and 5 meter resolution IfSAR (Interferometric Synthetic Aperture Radar) topography data (Jones and Grosse, 2013), and conducted a brief field reconnaissance in August, 2011. A prominent transgressive marine scarp lies a few km north of the study region (Williams et al., 1978).

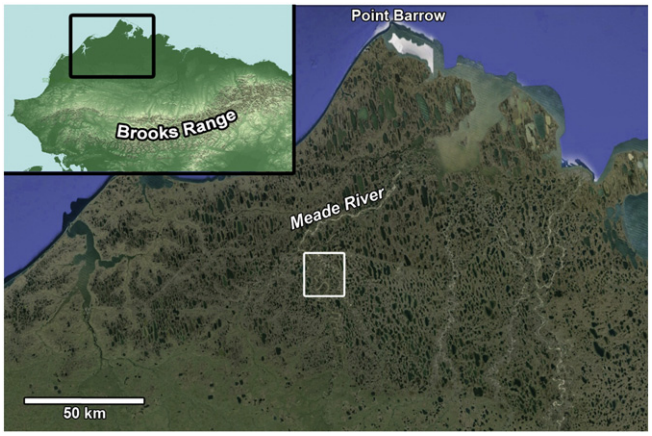

Fig. 10. The western North Coastal Plain of Alaska showing location of meander study area shown in Fig. 11. Inset shows general location of map. Thaw lakes occur primarily in Quaternary sediments of the unconsolidated sedimentary Gubik Formation (Black, 1964).

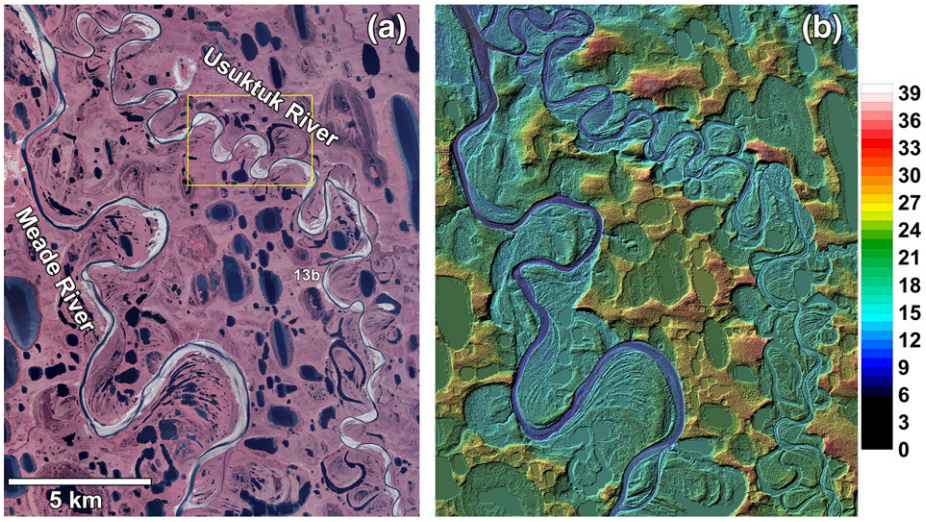

Fig. 11. Meander study area. (a) Digital Orthophoto Quadrangle mapping with reddish coloration on vegetated areas. Yellow box shows location of Fig. 12. (b) Shaded relief map with IfSAR elevations in color. Color scale in meters AMSL. Location of Fig. 13b shown in (a).

The Usuktuk River in the study region has a bankfull width of about 100 m with a valley gradient of about 0.0004 and a channel gradient about half that (Fig. 11b). Meander wavelength is about 1.84 km. Point bars are prominent as are scroll bars, and both are sandy. The channel bed was not visible during our visit, but appears to be sand-dominated. Strong winds from the east–northeast have eroded sand from point bars and have deposited prominent, poorly vegetated sand sheets and parabolic dunes on point bars and neighboring uplands (Fig. 12). Surrounding uplands are uneven in elevation, reflecting the original topography of the dunes which can extend locally 25 or more meters above river level. Point bars typically rise about 3–7 m above low water level, and are typically vegetated with dry dwarf shrub tundra beyond 200 m from the low-water river bank. Prominent scroll bars are often present (Fig. 12). The Usuktuk River has a highly sinuous planform (sinuosity ~ 2.6), but the presence of flood chutes across the point bars of several meander bends suggests that the river may be close to the meandering–braiding threshold (Fig. 12), or possibly they result from niveal seasonal fluctuations in discharge.

Based upon ubiquitous scroll bars on abandoned portions of the valley floor, the meandering pattern of the Usuktuk has probably been consistent over the life of the valley floor. Older parts of valley floor deposits, as well as oxbow lakes, are perched 2–6 m above modern point bar deposits. That suggests that the Usuktuk River has been slowly downcutting.

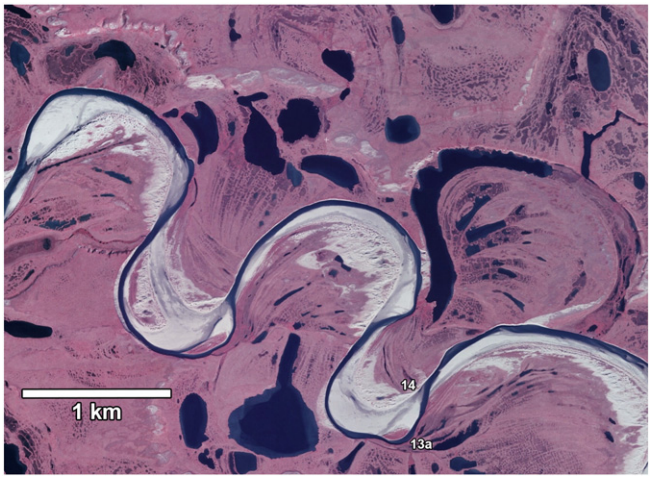

Fig. 12. Detail of study area in USGS DOQ map. Note sandy point bars, deposits of wind-blown sand eroded from point bars, thaw lakes, oxbow lakes, and scroll bars. See Fig. 10 for location. Numbers show locations of other figures.

The height and character of outer stream banks varies greatly. Where the river is eroding into the inactive dune deposits, the banks are as much as 20+ meters high, with largely bare sand and bank steepness near the angle of repose (Fig. 13b). In some locations dense fine roots permeate the sand, extending from shrubs capping the banks (Fig. 14). These roots exploit the seasonally unfrozen active layer on the stream banks. Where the stream is impinging into earlier point bar and overbank deposits, banks are typically 3–5 m high, generally strongly mantled with dense dwarf tundra and locally ~1 m willows (Fig. 13a). The banks are often undercut, and a vegetation mat often drapes over the undercut banks, or grows directly on the banks. The vegetation-mantled banks appear to offer appreciable resistance to fluvial erosion, apparently creating local bulges in the otherwise concave bank planforms.

During our August, 2011 visit, we saw no exposed massive ice on streambanks, either on the ground or from helicopter reconnaissance. Segregated ice as ice wedges is clearly present within both the Meade River dune deposits as well as in older point bar deposits because of abundant patterned ground and thaw lakes of various sizes. Thaw lakes develop from degradation of massive subsurface ice, e.g. Hinkel et al. (2003, 2005), Pelletier (2005), Hinkel and Hurd (2006), West and Plug (2008), Plug and West (2009), and Jorgenson et al. (2011).

We measured rates of bank erosion on outer meander bends of the Usuktuk River shown in Fig. 11 by comparative measurements on 1:40,000 scale aerial photography flown in 1955, with digital 1-m resolution DOQs flown in 2005. We selected 23 bank sections characterized by a generally smooth planform curvature. The aerial photography was georeferenced to a GIS database of the DOQs. We measured paired perpendicular distances from recognizable static features (patterned ground intersections, sharp oxbow and thaw lake margins, etc.) to the upper break in slope of stream banks on each dataset. We also measured planform curvature by fitting a circle to three digitized bank locations. Normalized planform curvatures (the assumed 100 m channel width divided by circle radius) ranged from 0.06 to 0.41, averaging 0.19. Apparent migration distance ranged from −2.2 m to 19.75 m, averaging 6.3 m (a mean migration rate of ~0.13 m year^{-1}, or 0.16 m year^{-1} discounting negative measurements). A regression of migration rate on curvature was statistically insignificant, but the measured mean rate of migration is significantly different from zero at the 95% level of significance. Four negative estimates of bank migration clearly indicate

Fig. 13. Views of meander cut banks. (a) Low bank eroded into relatively young fluvial deposits. Note strong shrub cover on upper surface, local sediment exposures, and varying degrees of bank mantling by vegetation mats collapsing and slumping onto the bank. (b) High bank (~20 m relative relief) cut into Gubik sand deposits. Slope angle close to angle of repose for sand. Note indications shallow regressive failures. Regressive failures appear to be limited to actively undercut sandy banks with appreciable vegetation cover. Older, vegetated bank scarp extends backward at right side of image. See Figs. 11 and 12 for locations.

the magnitude of measurement errors using the technique, which is likely about ±2 m, because of possible image distortion, difficulty in recognizing the upper bank location on the earlier black and white images, inter alia. We can conclude from this exercise that the very low bend rates of migration (~0.13 m year^{-1}) are much less than yearly active layer depths of thaw (~0.3–0.5 m), so that thermo-erosional potential is not a limiting factor, but rather rates of erosion are limited either because of fluvial sand transport capacity (particularly on the higher sandy banks which potentially contribute 20+ m^3 of sand per planform meter of bank for every 1 m of bank erosion) or cohesion introduced by bank vegetation. Another rough estimate of maximum rate of migration of the Usuktuk River results from noting that the maximum distance of migration recorded in scroll bars is about 2 km. The maximum age of thaw lakes near Barrow is about 5400 years BP (Hinkel et al., 2003). Meandering stream channels have developed across a number of the oldest thaw lakes, suggesting that 5400 years is a minimum age for establishment of drainage. This results in a long term maximum rate of migration of about 0.4 m year^{-1}, but the rate of migration is probably more in the range of what was measured photogrammetrically, particularly if the Usuktuk River is older and when considering average rather than maximum rates.

Despite the location of the Usuktuk River within the zone of continuous permafrost, we conclude that rates of bank erosion are limited by the necessity to erode and remove floodplain vegetation rather than permafrost ice cohesion.

Fig. 14. Dense network of fine plant roots extending from the shrubs beyond the crest of the bank. See Fig. 12 for location.

2.2. Quinn River, Nevada

Actively meandering rivers occur in scattered locations throughout the Great Basin region of the western United States. Several have developed within fine-grained lacustrine sediments of large late Pleistocene paleolakes, especially Lake Bonneville and Lake Lahontan. Examples include the Sevier River north of Sevier Lake in Utah, the Humboldt River upstream and downstream from the town of Winnemucca in Nevada, and the Quinn River (QR) in northwestern Nevada and southeastern Oregon (Fig. 15). Inactive sinuous channels also occur on the floor of Lake Bonneville near 40.3°N and 113.2°W (Oviatt et al., 2003). Most of the active sinuous rivers host appreciable phreatophytic vegetation on the banks and floodplains, including the headwater portions of the QR. The lower portions of the QR, however, are very sparsely vegetated yet the river is actively migrating, with evidence of a long history of meandering with cutoffs (Fig. 16). Vegetation is nearly absent from the convex eroding banks of the river, although scattered shrubs colonize portions of many of the higher inner, depositional banks (Figs. 6 and 17). Vegetation is clearly not a controlling factor in regulating the meandering of the QR. Thus, QR at the study site is a rare terrestrial example of a meandering channel in which the banks are free of

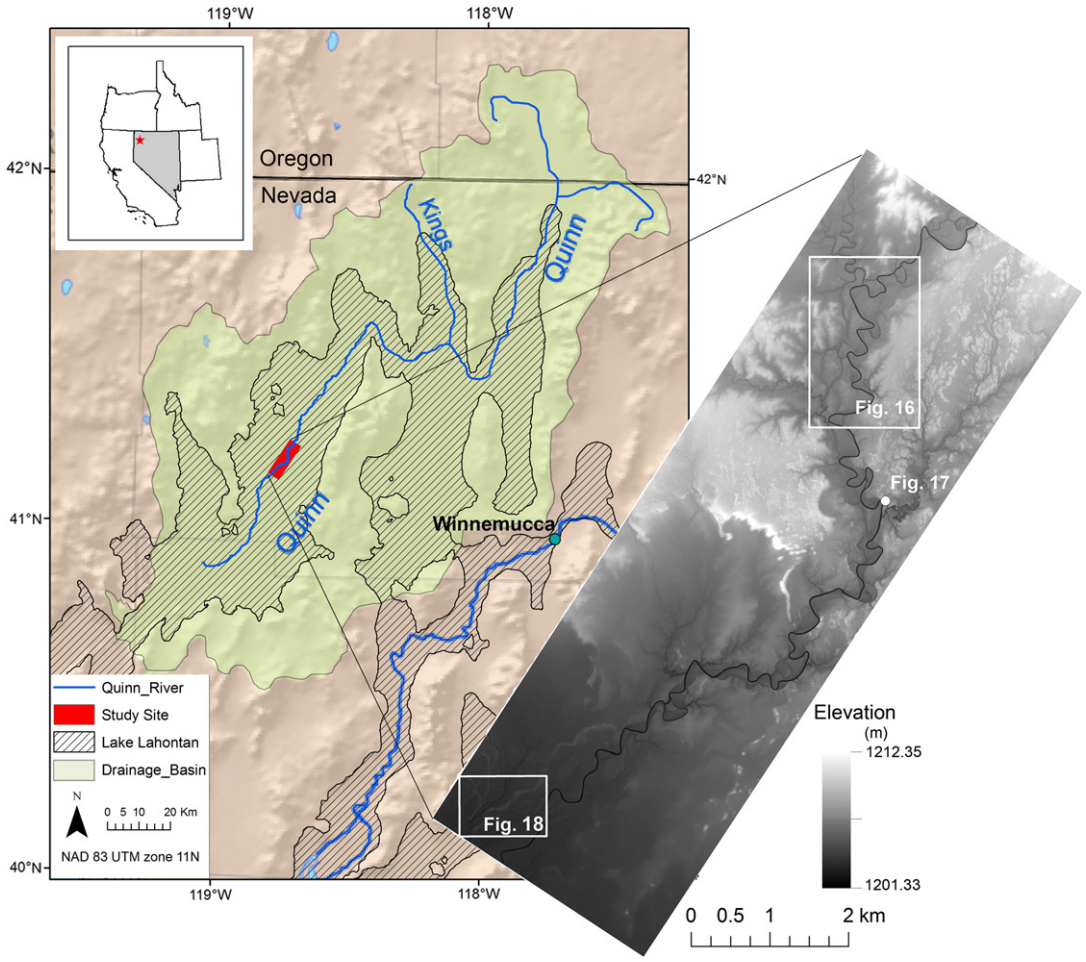

Fig. 15. Location map and a 1 m LiDAR DEM of the study area showing the drainage basin and a portion of the paleolake Lahontan. White boxes with numbers show locations of numbered figures.

appreciable vegetation but the channel is actively migrating. Aerial photographs taken over the last 50 years show at least three cutoff events within the study sites and some meander bends have migrated more than 40 m in 30 years. Mineral precipitates locally mantle the channel banks and floodplains (e.g., the light-toned areas near the top of Fig. 16a), potentially providing cohesion through chemical cementation. The sinuosity of the QR at the study site is about 1.8, which is within the range of the AD meanders. Cutoffs at the QR and in AD involve chute (Fig. 16b, location 1; Fig. 8) and neck cutoffs (Fig. 16b, location 3, Fig. 5a). Moreover, slightly inverted channels can be seen in the LiDAR DEM data at the QR (e.g., at the white arrow in Figs. 16b and 18). We examine below the possible roles of clay cohesion and chemical cementation in permitting a meandering pattern in the near absence of vegetation.

Observations reported here are based upon four field trips to the QR in a strongly meandering section (Fig. 16) from December, 2009 to October, 2011. We conducted GPS surveying, vane measurements of sediment shear resistance, penetrometer measurements, water jet tests of erodibility and critical shear stress for hydraulic erosion of sediments, grain size analyses, determination of major ions in distilled water and acid leaching of sediment samples, water chemistry, grain size analyses using a Coulter counter, and scanning electron microscopy of sediment samples. In addition, 1 m resolution LiDAR topography was collected for a 10 km reach of the river (e.g. Fig. 16).

The QR flows through the lacustrine deposits of paleo Lake Lahontan (Morrison, 1964; Reheis, 1999) across the center of the Blackrock Desert. The late Quaternary highstand of Lake Lahontan occurred between 14,500 and 13,000 years BP (Benson, 1991). The lake probably retreated from the study area by about 9500 years BP (Benson et al., 1990, 1992). It is likely that the QR began flowing across the abandoned lake bed as soon as the lake retreated. The abandoned meander deposits (e.g., Fig. 18) of the QR have not been dated, so the detailed history of meandering is unknown. Study of historical meander migration from aerial photography (Matsubara and Howard, 2014) shows that the rates of migration of meander bends are slow, averaging ~0.5 m/year, suggesting at least a few thousand years are recorded in the exposed meander deposits. Climate fluctuations have occurred on a variety of temporal scales throughout the late Pleistocene and Holocene of the Great Basin Region (e.g., Madsen et al. (2001), Tchakerian and Lancaster (2002), Balch et al. (2005), Briggs et al. (2005), Minckley et al. (2007), and Louderback and Rhode (2009)). Based, however, on the similar scale of old scroll bar patterns, the channel width of cutoff loops, and the meander wavelength of abandoned/avulsed channels, the effective flow regime of the river has not changed much during the period of recorded activity. It is likely that arid intervals are probably just not recorded in the fluvial deposits because erosional and depositional activity largely occurs during peak flows.

Flow in the QR is highly seasonal, being dominated by snowmelt from the mountainous headwaters in southeastern Oregon and northwestern Nevada (Fig. 15). Flow through the study area discharges into the Quinn River Sink, approximately 40 km downstream from the study site and evaporates. Discharge data are not available for the QR in Nevada. Estimating from the annual discharge data from the closest gauge station upstream of the study area, high discharges are typically observed from March through May (USGS Surface water data for gauge station 10353500). This station is located on the Quinn River

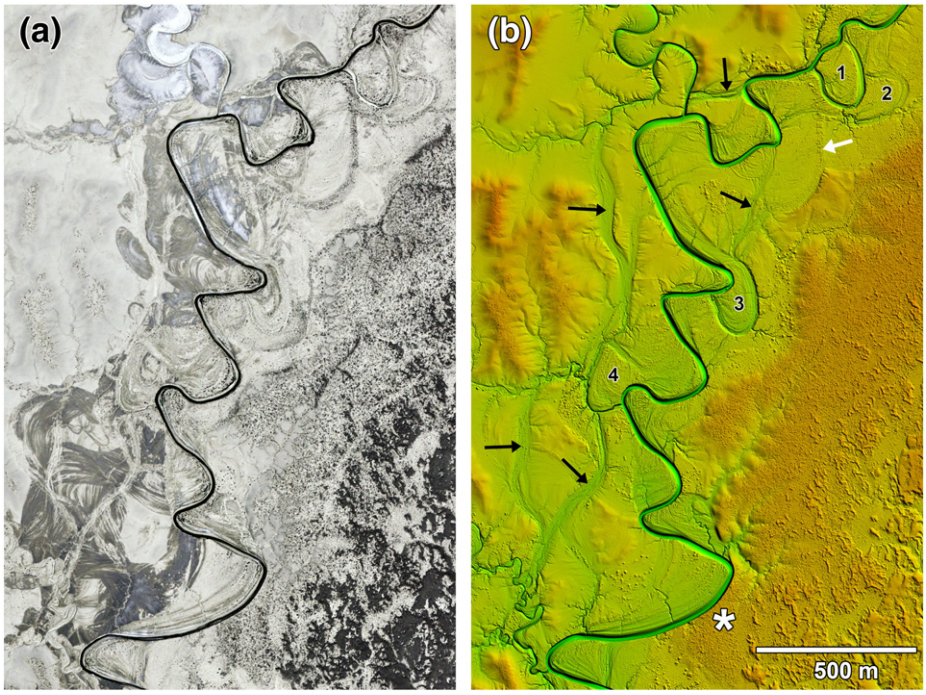

Fig. 16. Quinn River channel and fluvial features. (a) USDA Farm Service Orthophoto image taken in 2006, showing meander evolution traces in scroll bar and oblique accretion deposits. Light-toned areas near top of image, particularly along tributary are surface mineral crusts. Dark mottling at right is scattered shrubby vegetation. (b) National Center for Airborne Laser Mapping 1 m lidar topography. Total elevation range is about 6 m. Black arrows point to flood chutes on the Quinn River floodplain. The white arrow points to a paleochannel eroded into slight positive relief. Numbers refer to cutoffs. The "*" symbol is at a location where the river is cutting into Lake Lahontan clays. Elsewhere the channel is primarily reworking earlier floodplain deposits. Image centered at 41.21°N, 118.74°W.

Fig. 17. Mass wasting and fluvial features along a meander bend of the Quinn River, looking downstream. At this location the channel is eroding into Lake Lahontan sediments. Bank height on outer bank is 3.6 m and on the inner bank is 2.1 m. The right bank shows a typical expression of inner bank sediment deposited by oblique accretion. Short scarps on this bank reflect notching of bank during water level decline, presumably by wave action. The spring, 2011 high water was just above the highest notching and within the light-toned band with scattered low shrubs. Line of shrubby vegetation along the crest of the right bank marks an older scroll bar. The silty sand deposits comprising scroll bars are conducive to vegetation growth. Note that the prominent water mark on the left bank is well below the level of the 2011 high water, which probably reached to the break in slope on the bank. Mass wasting of small blocks from the steep upper bank has mantled the high water bank textures. A recessional water stage on the left bank is indicated by damp, light-toned smooth bank extending about 0.6 m above the present water level upper banks fail by block by block or by cantilever failure along tension cracks. Note incipient failure in foreground and numbered debris fans. Bank failure 4 occurred prior to the recessional level and its deposits below that level have been extensively reworked with the exception of a few partially eroded blocks at water level. Bank failure 3 may have occurred during the recessional water level and is partially reworked. Note that the disaggregation of the debris has produced a convexity in the bank at water level. Bank failure 2 may have had two separate events, being partially smoothed below the recessional water mark but with angular debris deposited after the water level had retreated to its present value. Bank failure 1 occurred after the recessional water level but while the river level was several centimeters above its present level. Image located at 41.192°N, 118.738°W and taken on October 15, 2011.

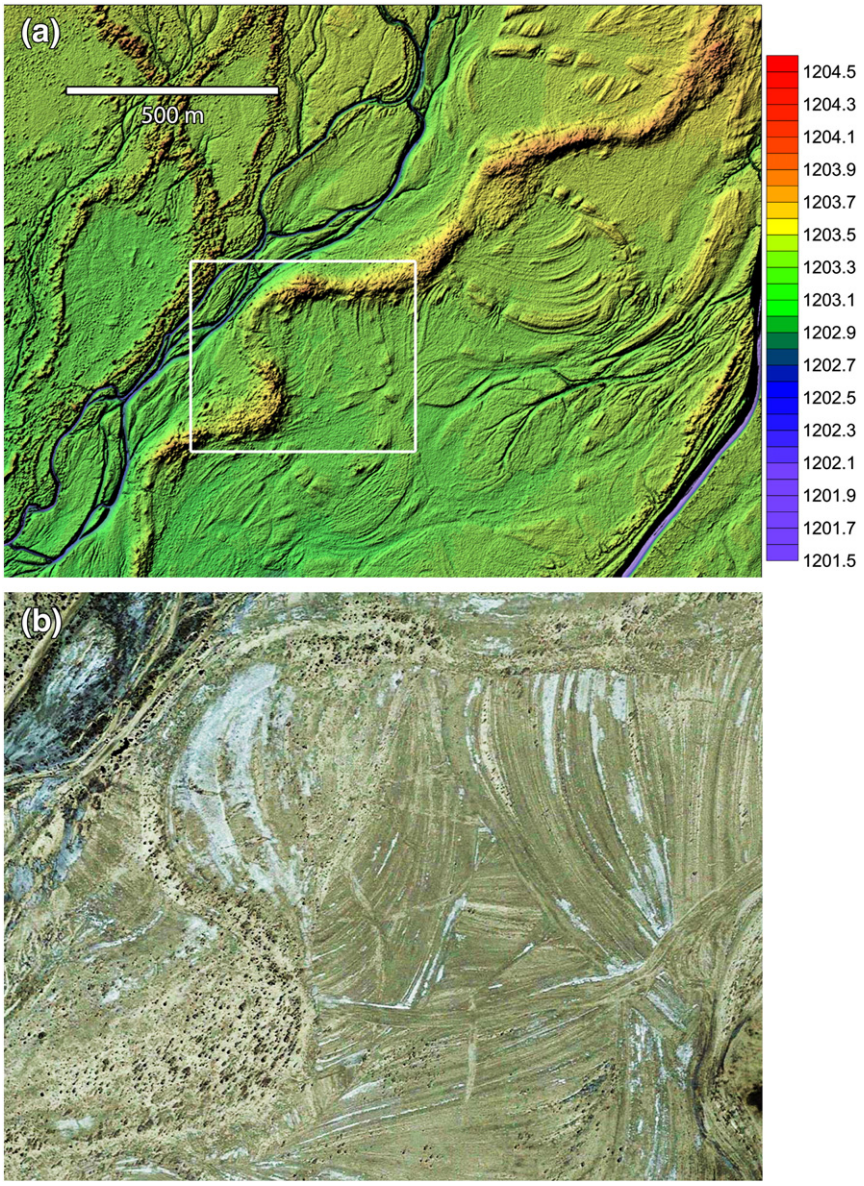

Fig. 18. Inverted abandoned channel on the floodplain of the Quinn River. (a) LiDAR elevation map. Elevation scale in m AMSL. Relative relief of inversion is less than 1 m. A short section of the Quinn River is at lower right. A tributary drainage crosses the floodplain at the upper left. Map is centered at 154.205°W, 41.155°N. (b) Detail of inverted channel and Quinn River oblique accretionary channel deposits. Note partial vegetation cover on inverted channel and near lack of vegetation on oblique accretion deposits. Whitish areas mantled by chemical crusts.
Image from Google Earth.

about 100 km upstream of the study area and discharge data were collected from 1949 to 1985. It should to be noted that in recent years the flow of the QR is being controlled for irrigation purposes and that large floods are rare. During summer and fall months, discharge through the river decreases to a trickle inferred to be sourced from groundwater. A heavy winter snowfall in 2010–2011 resulted in a broad flow peak during May and early June in the study area at about ¾-bankfull stage and flowing at approximately 0.42 m s^{-1}. Estimated discharge based on the flow velocity and the cross-sectional profile was 4.8 m^3 s^{-1}. We estimate bankfull discharge to be approximately 12 m^3 s^{-1} (Matsubara and Howard, 2014). The last major flood through the QR occurred around 1983. Small ephemeral channels sourced on the surrounding playa indicate that locally-sourced runoff occurs occasionally. Numerous flood chutes on the QR floodplain (Fig. 16b) indicate significant overbank flows occur. Flow modeling with the HEC-RAS program suggests overbank discharges creating flood chutes are probably in the range of 20 to 30 m^3 s^{-1} (Matsubara and Howard, 2014).

The QR has incised into clay-rich basin-center lacustrine deposits presumably dating to the late Pleistocene high water. Lateral incision by the river reveals exposures of these lake sediments, which are moderately consolidated with prismatic jointing. When directly exposed to water, however, the deposits slake rapidly into small aggregates. Several samples of lake sediments were analyzed for grain size distribution, revealing an average composition of about 60% silt and 40% clay, with minor sand (Fig. 19). Some exposures contained thin ash beds.

Because the QR flows across a paleolake surface, the channel gradient is very low (~0.00015). This prohibits coarse grained sediment from reaching the study area from the nearby mountains, making QR a mud (silt/clay)-dominated channel with the river banks and channel bed consisting almost exclusively of mud to fine sand. The grain size distribution indicates an average mud content of 78% (Matsubara, 2013) and that almost all of the samples have more than 41% mud content and some of the samples consist entirely of mud (Fig. 19). Silty sands are largely limited to overbank deposits as climbing ripples in scroll

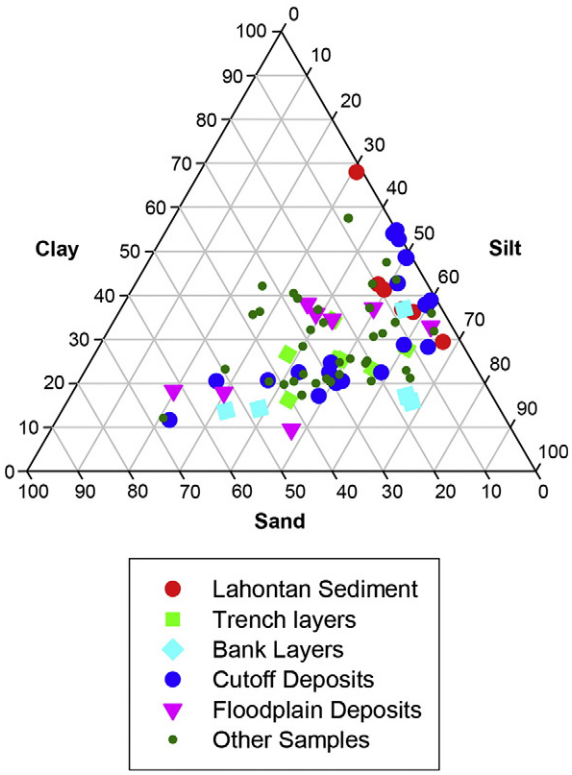

Fig. 19. Ternary diagram of sedimentary samples from the Quinn River study area. Grain size analysis using Coulter counter and dispersed samples. No components coarser than sand occurred in any sample. Lake Lahontan deposits are about 60% silt and 40% clay with little sand. The other sediment categories are samples of Quinn River deposits. Note that these can generally be modeled as Lake Lahontan deposits with added fine sand in varying amounts.

bars (Fig. 6), creating an upward-coarsening size grading to the fluvial sediments. Overall, however, variations in grain size distribution between the different depositional settings (channel perimeter, cutoff infill, and lake deposit) were small (Matsubara, 2013). Most QR sediment deposits have a clay/silt ratio of about 0.6 with varying amounts of fine sand (Fig. 19). This ratio suggests that the fluvial deposits are primarily reworked Lahontan lake deposits, with variable amounts of fine sand from other headwater sources. At numerous locations the QR is actively migrating laterally into Lake Lahontan sediment (e.g., at an "asterisk (*)" in Fig. 16b). Based on the study by Schumm (1963b) of vegetated meanders in the Midwestern U.S., the silt/clay content of QR sediment (original Lahontan clay and reworked fluvial deposits) is at the high end of the channels classified by Schumm with regard to the percentage silt and clay in the bed and banks.

Most meandering channels deposit a two-component vertical sequence: a lower, relatively cohesionless sand or gravel bedload and lateral accretion point-bar deposit overlain by finer, cohesive sediment deposited by vertical or oblique accretion (Wolman and Leopold, 1957; Allen, 1970; Bluck, 1971; Jackson, 1978; Nanson, 1980; Miall, 1996; Bridge, 2003; Page et al., 2003). Erosion of channel banks commonly occurs by slumping or toppling because of erosion of the less cohesive and largely unvegetated sediment in the lower part of channel banks from entrainment by river flow or seepage forces from ground water (e.g., Thorne and Tovey (1981), Thorne (1990), Thorne and Abt (1993), Thorne et al. (1998a,b), Simon et al. (1999), Wood et al. (2001), and Simon and Collison (2002)). This slumping and toppling of the cohesive upper banks usually just lowers the vegetated or cohesive layers onto the lower bank, which is often protected from further erosion until the slumped material is eroded by the flow (Thorne and Tovey, 1981; Osman and Thorne, 1988; Simon et al., 1999; Wood et al., 2001; Parker et al., 2011).

Processes of bank erosion and inner bank deposition along the QR are quite different from typical meandering channels because of the lack of a lower, cohesionless bedload and point bar stratum coupled with a negligible role of vegetation. The QR is an example of a suspended-load dominated river (Schumm, 1963b), in which the majority of deposition occurs by oblique accretion from suspension (Page et al., 2003). The term oblique refers to deposition occurring with components of vertical and lateral accretion. Channels dominated by suspended load deposition occur primarily in low-gradient channel systems, and often, as in this case, in streams crossing paleolacustrine deposits (Jackson, 1981; Brooks, 2003a,b). Page et al. (2003) recognize the possible case of channels depositing sediment solely by oblique accretion (e.g., Gibling et al. (1998)). Along the QR, the only important component of traction transport occurs during formation of climbing ripples in reworking fine sands deposited from suspension on scroll bars and scattered ripples on the channel bed formed by saltating mud aggregates (Fig. 20).

Rates of bank erosion appear to be limited by the ability of the river to entrain the cohesive sediment just above the river bed. Strongly undercut banks are essentially absent along the QR. Rather, the lower banks are commonly concave, progressing upward to convex slopes, or, along higher bank sections, transitioning to steep banks sometimes bordered downslope by angle-of-repose accumulation of sediment mass-wasted from the upper banks (Fig. 17). The mass-wasted debris is most common where the river is incising into Lake Lahontan sediment. Large slumps are essentially absent along river banks at the QR. Where upper bank slopes are steep, thin sheets of bank material fail along tensional fractures and spread debris on the lower slopes. Debris shed onto lower river bank slopes is reworked by subsequent high flows. The dry clay expands and rapidly slakes into small aggregates when wetted, contributing to rapid mobilization. The dense, prismatic fragments mass wasted from the Lake Lahontan deposits are particularly susceptible to slaking. These observations indicate that the rate of outer bank erosion is not strongly controlled by erosional resistance of the upper banks. An indirect control of the rate of erosion by bank height does exist, however, because higher banks cutting into Lake Lahontan sediment erode more slowly, probably because the slaking of the mass-wasted debris adds a layer of clay to the lower banks (Fig. 17).

The lower bank of the river, within about 0.6 m (measured vertically) of low water levels, remains constantly damp by water contributed by a near-surface groundwater table. Sediment less than about 0.3 m from low water is cohesive and slippery. Damp clay, though seemingly counterintuitive, is difficult to entrain. Dry clay, on the other hand, expands and slakes into small aggregates immediately when the flow

Fig. 20. A photo of dunes on the Quinn River bed created by aggregated clays. Insert image shows some of the large flocs forming the dunes.

comes through in the spring and the slaking process contributes to rapid erosion. This is supported by the data from submerged jet shear tests (Hanson and Simon, 2001; Hanson and Cook, 2004) indicating that channel banks of the QR are very erodible at the top and gradually become less erodible near the water edge.

It is uncertain the degree to which just hydraulic stress versus wetting and swelling control the rate of erosion. Even during the high flows observed in the spring of 2011 (estimated bed shear stress 0.98 Pa), QR was still only modestly muddy and the collected water sample did not contain much sediment demonstrating that ¾ bankfull stage is still not enough to massively entrain wet silt/clay sediments. Estimated shear stress for bankfull conditions is 1.5 Pa.

In addition to abundant mud, ion chromatography analysis indicated that salts are found ubiquitously in sediments and as well as in river water (Table 2) (Matsubara, 2013). The presence of less soluble divalent ions (e.g., Ca^{2+} and Mg^{2+} species) suggests that chemical cementation could be providing cohesion to the channel banks. This was proven not to be the case at the QR, however, when and scanning electron microscope (SEM) images showed no evidence of precipitate crystals binding sediments together (Fig. 21). The images show that sediment particles are typically draped (wrapped) with clay (Matsubara, 2013). Salt crystals (Ca, K, Na species) were found in SEM samples as well, but not as abundant/uniformly as mud drapes. Also because the sediment samples had to be completely dried to coat samples with carbon, it is inevitable for salt crystals to grow as the water evaporates. Thus, the salt crystals (~1 μm) we see in the SEM images may not be representative of natural conditions.

Although no evidence exists of chemical cementation of the QR sediments, the high solute content of river water may still play an important role in providing bank cohesion. Dissolved solutes encourage flocculation and settling of fine sediment. This was illustrated by simple rate of deposition tests in graduated cylinders (Fig. 22). Representative QR sediment mixed in distilled (DI) water took much longer to settle than those in saline water (Matsubara, 2013). All sediment in a solution with a salt concentration equivalent to sea water and with solute concentrations representative of the QR at low flow conditions (Table 2, rows 1 and 3) settled within 40 min. All of the sediment settled after 8 h in a solution with salt concentration equal to the QR at high flow (Table 2, row 2). Conversely, sediment in DI water remained partially in suspension after 24 h. Fine sediments in DI water with dispersant remained in suspension even after a week. It should be noted that the physical agitation in the turbulent flow can break apart flocculated clay particles and place an upper limit to floc growth.

The flocculation effect was observed in the field when river water sample was collected during the spring, 2011 high flow (5 $m^3\ s^{-1}$) event. The suspended sediment within the water sample settled to the bottom of the container within a few minutes. Also, large aggregates were transported as bedload during high flows, forming ripples and dunes locally on the channel bed (Fig. 18). Flocculation allows clay, which would otherwise be removed from the river as wash load, to be rapidly redeposited, which then collapse to form dense, cohesive drapes on the bank. During falling stages, clay/silt drapes occur on the accreting inner banks and also on the eroding outer banks, providing a coating that must be eroded in a subsequent high flow stage before net bank erosion can occur. The flocculated sedimentation followed by cohesion development presumably also interacts with flow detachment to regulate the river width to be narrow enough to maintain a meandering planform.

Some channel segments of the QR abandoned by avulsion have become inverted by less than 1 m (Fig. 18). Portions of these segments are separated from the current channel by more than 500 m and are unlikely to have infilled by backwater or overbank sedimentation, as happens for local cutoffs (e.g. Fig. 16b). We infer that the abandoned channels were infilled by aeolian sand transport, which was then modestly cemented by salts leached from finer silt and dust codeposited with the sand. They also host a denser vegetation cover than the surrounding clay-rich sediment, probably contributing to erosional resistance and possibly encouraging additional aeolian sand deposition.

The active meandering of the QR in a mud-rich but vegetation-poor environment indicates that sufficient bank cohesion permitting meandering can be facilitated by mud deposition encouraged by flocculation in a solute-rich environment.

Table 2
Major ion concentrations (mmol/L) in Quinn River water samples.[a]

Sample	Na^+	K^+	Mg^{2+}	Ca^{2+}	Cl^-	SO_4^{2-}
May, 2010 at low/ponded water	192.3	0.9	1.4	0.6	128.6	12.7
May, 2011 at 5 $m^3\ s^{-1}$	3.5	0.3	0.4	1	0.9	0.4
October, 2011 at low water	92.7	0.5	0.1	0.3	55.6	7.9

[a] Dissolved CO_2 species were not measured, and probably largely account for charge imbalances.

3. Discussion

We have explored three possible mechanisms that could contribute to the bank cohesion required for channels to meander in the absence of appreciable vegetation cover: permafrost, abundant clays, and chemical cementation. The effect of ice on bank cohesion was studied at the Usuktuk River in Alaska. Control of meander pattern and bank migration by ice in bank materials, however, does not appear to be a dominant factor for the Usuktuk River, despite its location in perennial permafrost with associated cold-climate features such as patterned ground and thaw lakes indicating the subsurface presence of massive ground ice. Vegetation appears to have a strong control on meander evolution of the Usuktuk, which makes it unlikely to be a representative analog to AD. One caveat is that this fieldwork was conducted in August. It may be possible that bank retreat occurs only during the high flows when permafrost starts to thaw, allowing temporary exposure of permafrost. In addition, we have identified no obvious periglacial landforms such as patterned ground or thaw depressions exposed in the fluvial or MFF deposits in the AD region. A possibly important further difference is that the AD channels were aggrading during meander evolution, whereas the Usuktuk River appears to be slowly incising. Finally, in a larger context, we note that, in the High Arctic north of the zone of coherent tundra vegetation, meandering channels are rare or absent (Vandenberghe, 2001). Larger Arctic rivers which locally expose permafrost in the banks do not exhibit the highly sinuous meandering characteristic of AD meanders. We, thus, find no compelling evidence from terrestrial analogs to support ice cementation as a controlling factor in the development of the AD meanders.

Our study at the QR showed that meandering rivers can form in regions with sparse vegetation with abundant mud and chemical precipitates as possible alternate sources of cohesion. The SEM images show that sediment particles are draped (wrapped) with clay and that it is mud that is binding sediments together. Although analysis of leachates from sediment samples showed high concentrations of soluble salts and acid-released carbonates, they do not appear to be a significant source of cohesion. Abundant efflorescences of salts from evaporation of water migrating to the surface by capillary flow cover extensive areas of QR sediments (e.g., Figs. 16a and 18). These surface coatings, however, do not create appreciable cohesion in the underlying sediments. We conclude that high mud content rather than chemical cementation is the dominant source of sediment cohesion.

Bank cohesion at the QR is indirectly controlled by the effect of high solute content on flocculation and deposition of mud aggregates. Various types of salts, particularly chlorides and sulfates, are observed on Mars (Bibring et al., 2006; Christensen et al., 2007; Osterloo et al., 2008). An examination of CRISM/OMEGA spectral data, however, reveals no definitive detection of clays at AD region. The resolutions of the spectral datasets are coarse, however, and no clays were detected from the orbiter at the site visited by the Mars Science Laboratory

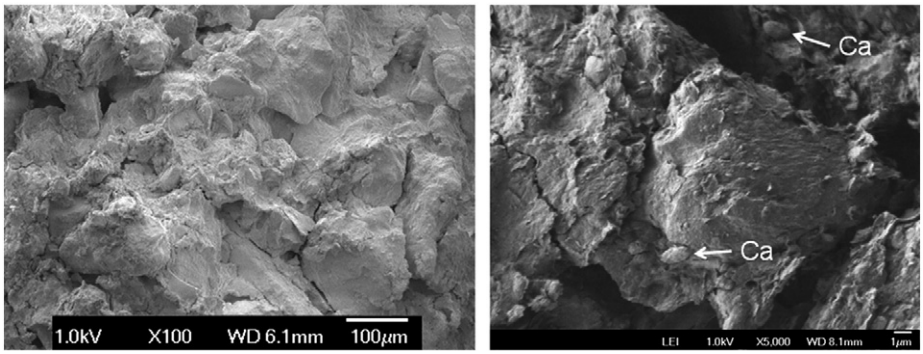

Fig. 21. SEM images taken at 100× (left) and 5000× (right) magnification both showing Quinn River sediments coated with clay. Individual salt (Ca) crystals were observed as well.

rover that has ~20% clay content (Bristow et al., 2013). The AD region shows evidence of extensive aeolian activity (Zimbelman and Griffin, 2010). Consequently, the lack of hydrated mineral signature at this site may result from the dust cover (Ruff and Christensen, 2002).

One counter argument for the QR as a potential analog for Martian meanders is that most of the meanders found on Mars are inverted. Inverted channels often form when bed sediment, which is usually coarser than the overlying finer floodplain sediment, is chemically cemented and then subsequently exposed by erosion of the finer surrounding materials (e.g., Williams (2007); Williams et al. (2009)). Initially cohesionless bed sediment is commonly favored for subsequent cementation because of its permeability which encourages fluid migration. The coarse-grained bedload and point bar sediments are, however, lacking at QR. Such channel bed deposits appear to comprise the channel material exposed in the AD meanders (e.g., Fig. 5). Aeolian infilling and cementation is not a likely explanation for the preservation of the AD meanders shown in Fig. 5 which express a continuous history of channel migration. Aeolian infilling followed by cementation, however, could potentially explain the thin, multilevel inverted meanders shown in Fig. 3 and the slightly inverted abandoned channels at the QR (Fig. 18).

The role of moisture content and duration of bank submergence on erosion rate is a topic that needs to be explored further. Although the QR is composed mainly of mud, water during moderately high flows was relatively clear. This implies that QR did not reach the threshold flow velocity to rapidly erode bank sediment. Wet clays are harder to

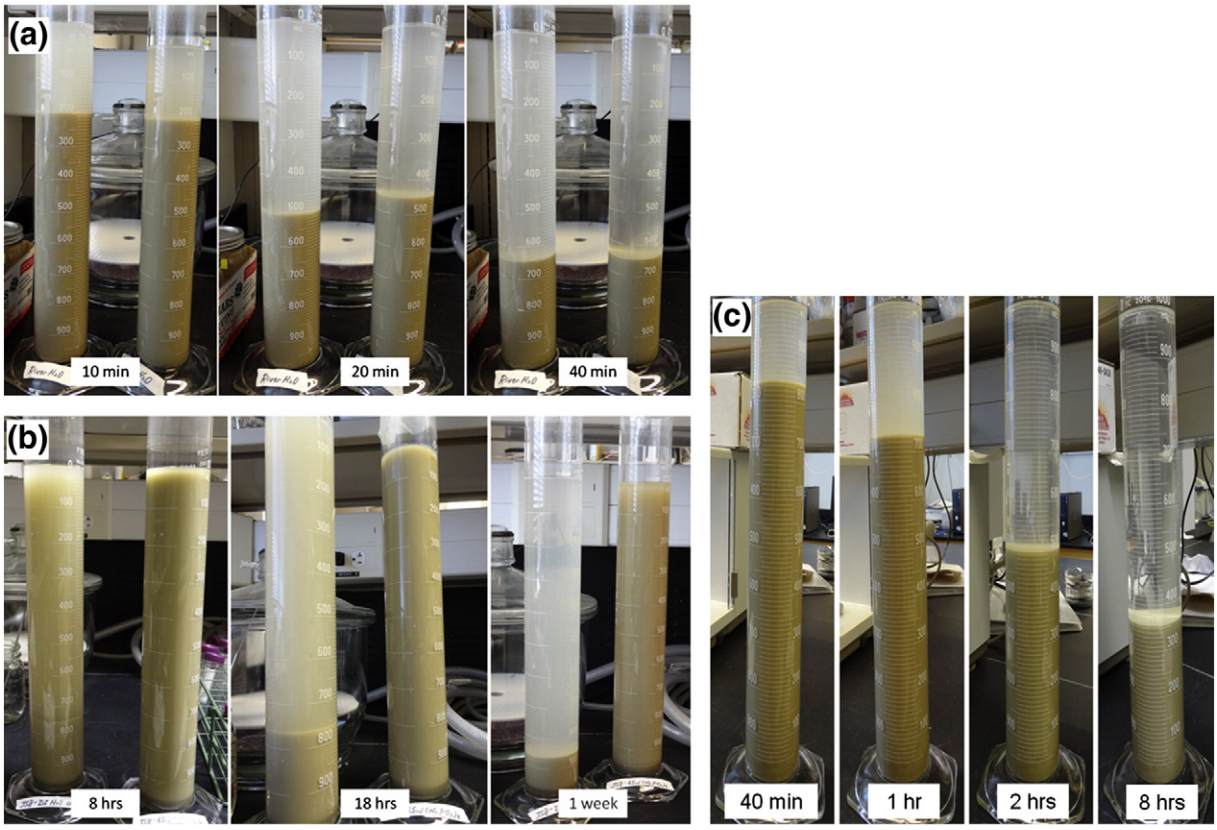

Fig. 22. Sediment settling experiments for Quinn River sediment in different solutions. Deposition rates for sample in solute concentration equivalent to that of Quinn River during ponded condition (a, left cylinder) and sea water (a, right cylinder) were about the same and were much faster than the other three solutions. Sample mixed in DI water only (b, left cylinder), DI water + dispersant (b, right cylinder) took much longer to settle compared to those placed in saline water. Solute concentration equivalent to that of Quinn River during high flow (c) was enough to accelerate deposition.

entrain than dry clay, and (wet) clay that is armoring the channel bank might require to be submerged for some length of time before losing its plasticity sufficiently to start moving.

Although most terrestrial meandering rivers have banks and floodplains that are strongly vegetated, bank cohesion and point-bar sedimentation in some rivers might be dominated by the mud content. This is suggested by the strong correlations between mud content, channel width, and sinuosity noted by Schumm (1960, 1963a). These observations, however, should be tempered by the indirect effects of sediment characteristics on vegetation density and the role of vegetation in encouraging fine sediment deposition. Nonetheless, further investigation of the direct contribution of mud to bank cohesion and point bar sedimentation in fine-grained meandering systems is warranted.

4. Conclusions

The paleo-meanders in the Aeolis Dorsa region on Mars present a compelling argument that meandering channels can develop in the absence of vegetation. We have reviewed the factors producing cohesive stream banks permitting meandering versus braided channels and studied two possible terrestrial analog sites: the permafrost region in northern Alaska and mud and solute rich Black Rock Desert, Nevada.

The arctic Usuktuk and the AD meanders share an apparently fine-textured parent material, similar channel dimensions, low channel gradients, and sinuous planforms with meander migration and occasional cutoffs. During our visit, however, no exposure of massive ice occurred on streambanks. The banks are often undercut, and a vegetation mat often drapes over the undercut banks, or grows directly on the banks. Vegetation appears to have a strong control on meander evolution of the Usuktuk, which is unlikely to have an analog in AD. Also no obvious periglacial landforms, such as patterned ground or thaw depressions, are exposed in the fluvial or MFF deposits in the AD region.

The Quinn River in Nevada is a mud dominated system with grain size distribution of at least 41% silt/clay at all locations (channel bed, banks, and floodplains). Ion chromatography analysis and SEM images also showed presence of salts in abundance in sediments and river water. Although these images showed no evidence of precipitate crystals binding sediments together, the high dissolved ion concentrations in the water and in QR sediment have an important influence on sediment deposition. Hydrometer settling experiments clearly showed that presence of salt in the river water encourages the deposition of fine sediment aggregates. If it were not for the saline river water, mud would remain suspended and transported downstream to the terminal playa. Dissolved solutes encourage rapid deposition and flocculation and settling of fine sediment. In the field, ripples and dunes composed of large mud aggregates were locally found on the channel bed. Our study at the Quinn River showed that in the absence of vegetation, bank cohesion is provided by mud with salts aiding flocculation. Both of these elements are also likely present in rivers on Mars.

Acknowledgments

This research was funded by a NASA Mars Fundamental Research grant to the University of Virginia, with Howard as a PI and Williams and Burr as Co-I's. LiDAR topographic mapping of the Quinn River was funded by a seed grant to Y. Matsubara from the National Center for Airborne Laser Mapping. We acknowledge the support of the U.S. Bureau of Land Management at the Winnemucca office in securing permits to work in the Quinn River Wilderness Area and at the Fairbanks, Alaska office for our study in Alaska. In addition to listed authors, field assistance at the Quinn River study was provided by Christian Braudrick, Alex Morgan, Sarah Drummond, Stan Dunford-Jackson, and Marisa Palucis. Carolyn Dufurrena provided extensive local information and local facilities. Davy Kern and Quinton Boyles supplied pack services to the Quinn River site. Gary Quarles provided helicopter service in Alaska, and the Barrow Alaska Science Consortium provided local logistics and permitting help.

References

Allen, J.R.L., 1970. A quantitative model of grain size and sedimentary structures in lateral deposits. Geol. J. 7, 129–146.
Allmendinger, N.E., Pizzuto, J., Potter, N., Johnson, T., Hession, W.C., 2005. Influence of riparian vegetation on stream width, eastern Pennsylvania, USA. Geol. Soc. Am. Bull. 117 (1/2), 229–243.
Andrews, E.D., 1984. Bed-material entrainment and hydraulic geometry of gravel-bed rivers in Colorado. Geol. Soc. Am. Bull. 95 (3), 371–378.
Balch, D.P., Cohen, A.S., Schnurrenberger, D.W., Haskell, B.J., Valero Garces, B.L., Beck, J.W., Cheng, H., Edwards, R.L., 2005. Ecosystem and paleohydrological response to Quaternary climate change in the Bonneville Basin, Utah. Palaeogeogr. Palaeoclimatol. Palaeoecol. 221, 99–122.
Benson, L.V., 1991. Timing of the last highstand of Lake Lahontan. J. Paleolimnol. 5 (2), 115–126.
Benson, L.V., Currey, D.R., Dorn, R.I., Lajoie, K.R., Oviatt, C.G., Robinson, S.W., Smith, G.I., Stine, S., 1990. Chronology of expression and contraction of four Great Basin lake systems during the past 35,000 years. Palaeogeogr. Palaeoclimatol. Palaeoecol. 78 (3–4), 241–286.
Benson, L., Currey, D., Lao, Y., Hostetler, S., 1992. Lake-size variations in the Lahontan and Bonneville Basins between 13000 and 9000 14C yr BP. Palaeogeogr. Palaeoclimatol. Palaeoecol. 95 (1–2), 19–32.
Bibring, J.-P., Langevin, Y., Mustard, J.F., Poulet, F., Arvidson, R.E., Gendrin, A., Gondet, B., Mangold, N., Pinet, P., Forget, F., 2006. Global mineralogical and aqueous Mars history derived from OMEGA/Mars Express data. Science 312 (5772), 400–404. http://dx.doi.org/10.1126/science.1122659.
Black, R.F., 1964. Gubik Formation of Quaternary age in northern Alaska. U.S. Geol. Surv. Prof. Pap. 302-C, 50–91.
Bluck, B.J., 1971. Sedimentation in the meandering River Endrick. Scott. J. Geol. 7, 93–138.
Bradley, B.A., Sakimoto, S.E.H., Frey, H., Zimbelman, J.R., 2002. Medusae Fossae Formation: new perspectives from Mars Global Surveyor. J. Geophys. Res. 108 (E8). http://dx.doi.org/10.1029/2001JE001537.
Braudrick, C.A., Dietrich, W.E., Leverich, G.T., Sklar, L.S., 2009. Experimental evidence for the conditions necessary to sustain meandering in coarse-bedded rivers. Proc. Natl. Acad. Sci. 106, 16,936–916,941. http://dx.doi.org/10.1073/pnas.0909417106.
Bridge, J.S., 2003. Rivers and Floodplains: Forms, Processes, and Sedimentary Record. Blackwell Science, Oxford.
Briggs, R.W., Wesnousky, S.G., Adams, K.D., 2005. Late Pleistocene and late Holocene lake highstands in the Pyramid Lake subbasin of Lake Lahontan, Nevada, USA. Quat. Res. 64 (2), 257–263.
Bristow, T., Blake, D.F., Bish, D.L., Vaniman, D., Ming, D.W., Morris, R.V., Chipera, S., Rampe, E.B., Farmer, J.D., Treiman, A.H., Downs, R., Morrison, S., Achilles, C., Des Marais, D.J., Crisp, J.A., Sarrazin, P., Morookian, J.M., Grotzinger, J.P., Team, M.S., 2013. The first X-ray diffraction patterns of clay minerals from Gale crater. American Geophysical Union Fall Meeting, Abstract P23B-1786.
Brooks, G.R., 2003a. Alluvial deposits of a mud-dominated stream: the Red River, Manitoba, Canada. Sedimentology 50, 441–458.
Brooks, G.R., 2003b. Holocene lateral channel migration and incision of the Red River, Manitoba, Canada. Geomorphology 54, 197–215.
Burr, D.M., 2011. Sedimentology in a reduced-gravity environment: submarine analogs for streamlined forms on Mars. Geology 39 (7), 703–704.
Burr, D.M., Carling, P.A., Beyer, R.A., Lancaster, N., 2004. Flood-formed dunes in Athabasca Valles, Mars: morphology, modeling, and implications. Icarus 171 (1), 68–83.
Burr, D.M., Enga, M.-T., Williams, R.M.E., Zimbelman, J.R., Howard, A.D., Brennand, T.A., 2009. Pervasive aqueous paleoflow features in the Aeolis/Zephyria Plana Region, Mars. Icarus 200, 52–76.
Burr, D.M., Williams, R.M.E., Wendell, K.D., Chojnacki, M., Emery, J.P., 2010. Inverted fluvial features in the Aeolis/Zephyria Plana region, Mars: formation mechanism and initial paleodischarge estimates. J. Geophys. Res. 115, E07011. http://dx.doi.org/10.1029/02009JE003496.
Carter, L.D., 1981. A Pleistocene sand sea on the Alaskan Arctic coastal plain. Science 211 (4480), 381–383.
Carter, L.M.E.A., 2009. Shallow radar (SHARAD) sounding observations of the Medusae Fossae Formation, Mars. Icarus 199, 295–302.
Charlton, F.G., Brown, P.M., Benson, R.W., 1978. The hydraulic geometry of some gravel rivers in Britain. Hydraulics Research Station Report, IT 180.
Christensen, P.R., Osterloo, M., Hamilton, V., Edwards, C., Wray, J., Anderson, F.S., 2007. Aqueous Mineral Deposits in an Ancient, Channeled, Equatorial Terrain, Mars, 2nd Mars Science Laboratory Landing Site Workshop.
Costard, F., Dupeyrat, L., Gautier, E., Carey-Gailhardis, E., 2003. Fluvial thermal erosion investigations along a rapidly eroding river bank: application to the Lena River (Central Siberia). Earth Surf. Process. Landf. 28 (12), 1349–1359.
Cotter, E., 1978. Evolution of fluvial style, with special reference to the central Appalachian Paleozoic. In: Miall, A.D. (Ed.), Fluvial Sedimentology. Canadian Society of Petroleum Geologists, Calgary, Canada, pp. 361–383.
Crosato, A., Mosselman, E., 2009. Simple physics-based predictor for the number of river bars and the transition between meandering and braiding. Water Resour. Res. 45, W03424. http://dx.doi.org/10.1029/02008WR007242.
Dade, W.B., 2000. Grain size, sediment transport and alluvial channel pattern. Geomorphology 35 (1–2), 119–126.
Davies, N.S., Gibling, M.R., 2010a. Cambrian to Devonian evolution of alluvial systems: the sedimentological impact of the earliest land plants. Earth Sci. Rev. 98, 171–200.

Davies, N.S., Gibling, M.R., 2010b. Paleozoic vegetation and the Siluro-Devonian rise of fluvial lateral accretion sets. Geology 38 (1), 51–54.
Davies-Colley, R.J., 1997. Stream channels are narrower in pasture than forest. N. Z. J. Mar. Freshw. Resour. 31, 599–608.
Dietrich, W.E., Perron, J.T., 2006. The search for a topographic signature of life. Nature 439, 411–418. http://dx.doi.org/10.1038/nature04452.
Engelund, F., Skovgaard, O., 1973. On the origin of meandering and braiding in alluvial streams. J. Fluid Mech. 57 (2), 289–302.
Eriksson, P.G., Condie, K.C., Tirsgaard, H., Mueller, W.U., Allermann, W., Miall, A.D., Aspler, L.B., Catuneanu, O., Chiarenzelli, J.R., 1998. Precambrian clastic sedimentation systems. Sediment. Geol. 120 (1–4), 5–53.
Federici, B., Paola, C., 2003. Dynamics of channel bifurcations in non cohesive sediments. Water Resour. Res. 39 (ESG3), 1–15.
Ferguson, R.I., 1987. Hydraulic and sedimentary controls of channel pattern. In: Richards, K.S. (Ed.), River Channels: Environment and Process. Blackwell, Oxford, pp. 129–158.
Fralick, P., Zaniewski, K., 2012. Sedimentology of a wet, pre-vegetation floodplain assemblage. Sedimentology 59, 1030–1049.
Frederici, B., Seminara, G., 2003. On the convective nature of bar instability. J. Fluid Mech. 487, 125–145.
Fredsoe, J., 1978. Meandering and braiding of rivers. J. Fluid Mech. 84 (4), 609–624.
Friedkin, J.F., 1945. A laboratory study of the meandering of alluvial rivers. U.S. Waterways Engineering Experimental Station, Vicksburg.
Friedman, J.M., Osterkamp, W.R., Lewis Jr., W.M., 1996. The role of vegetation and bed-level fluctuations in the process of channel narrowing. In: Osterkamp, W.R., Hupp, C.R. (Eds.), Fluvial Geomorphology and Vegetation. Elsevier, Amsterdam, pp. 341–351.
Fugita, Y., 1989. Bar and channel formation in braided streams. In: Ikeda, S., Parker, G. (Eds.), River Meandering. Water Resources Monograph 12. American Geophysical Union, Washington, D.C., pp. 417–462.
Fukuoka, S., 1989. Finite amplitude development of alternate bars. In: Ikeda, S., Parker, G. (Eds.), River Meandering. Water Resources Monograph 12. American Geophysical Union, Washington, D.C., pp. 417–462.
Gautier, E., Brunstein, D., Costard, F., Lodina, R., 2003. Fluvial dynamics in a deep permafrost zone — the case of the middle Lena river (Central Siberia). In: Phillips, Springerman, Arenson (Eds.), Permafrost. Swets & Zeitlinger, Lisse, pp. 271–275.
Gibling, M.R., Nanson, G.C., Maroulis, J.C., 1998. Anastomosing river sedimentation in the Channel Country of central Australia. Sedimentology 45, 595–619.
Graf, W.L., 1978. Fluvial adjustments to the spread of tamarisk in the Colorado Plateau region. Geol. Soc. Am. Bull. 89, 1491–1501.
Gran, K.B., Paola, C., 2001. Riparian vegetation controls on braided stream dynamics. Water Resour. Res. 37, 3275–3283.
Hanson, G.J., Cook, K.R., 2004. Apparatus, test procedures, and analytical methods to measure soil erodibility in situ. Appl. Eng. Agric. 20 (1), 455–462.
Hanson, G.J., Simon, A., 2001. Erodibility of cohesive streambeds in the loess area of the Midwestern USA. Hydrol. Process. 15 (1), 23–38.
Hession, W.C., Pizzuto, J.E., Johnson, T.E., Horwitz, R.J., 2003. Influence of bank vegetation on channel morphology in rural and urban watersheds. Geology 31 (2), 147–150.
Hey, R.D., Thorne, C.R., 1986. Stable channels with mobile gravel beds. J. Hydraul. Eng. 112, 671–689.
Hickin, E.J., 1984. Vegetation and river channel dynamics. Can. Geogr. 26 (2), 111–126.
Hinkel, K.M., Hurd Jr., J.K., 2006. Permafrost destabilization and thermokarst following snow fence installation, Barrow, Alaska, U.S.A. Arct. Antarct. Alp. Res. 38 (4), 530–539.
Hinkel, K.M., Eisner, W.R., Bockheim, J.G., Nelson, F.E., Peterson, K.M., Dai, X., 2003. Spatial extent, age, and carbon stocks in drained thaw lake basins on the Barrow Peninsula, Alaska. Arct. Antarct. Alp. Res. 35 (3), 291–300.
Hinkel, K.M., Frohn, R.C., Nelson, F.E., Eisner, W.R., Beck, R.A., 2005. Morphometric and spatial analysis of thaw lakes and drained thaw lake basins in the western Arctic Coastal Plain, Alaska. Permafr. Periglac. Process. 16 (4), 327–341.
Howard, A.D., 1996. Modelling channel evolution and floodplain morphology. In: Anderson, M.G., Walling, D.E., Bates, P.D. (Eds.), Floodplain Processes. John Wiley & Sons, Chichester, pp. 15–62.
Howard, A.D., Moore, J.M., Irwin III, R.P., Dietrich, W.E., 2007. Boulder transport across the Eberswalde delta. Lunar and Planetary Sci. Conf. XXXVIII, Abstract 1168.
Howard, A.D., Moore, J.M., Dietrich, W.E., Perron, J.T., 2008. Martian gullies: morphometric properties and flow characteristics. Lunar and Planetary Institute Conference Abstracts, p. 1629.
Huang, H.Q., Nanson, G.C., 1997. Vegetation and channel variation: a case study of four small streams in southeastern Australia. Geomorphology 18, 237–249.
Huang, H.Q., Nanson, G.C., 1998. The influence of bank strength on channel geometry: an integrated analysis of some observations. Earth Surf. Process. Landf. 23, 865–876.
Huisink, M., De Moor, J.J.W., Kasse, C., Virtanen, T., 2002. Factors influencing periglacial fluvial morphology in the northern European Russian tundra and taiga. Earth Surf. Process. Landf. 27 (11), 1223–1235.
Hynek, B.M., Phillips, R.J., Arvidson, R.E., 2003. Explosive volcanism in the Tharsis region: global evidence in the Martian geologic record. J. Geophys. Res. Planets 108 (E9), 5111. http://dx.doi.org/10.1029/2003JE002062.
Irwin III, R.P., Craddock, R.A., Howard, A.D., 2005a. Interior channels in Martian valley networks: discharge and runoff production. Geology 33, 489–492.
Irwin III, R.P., Maxwell, T.A., Howard, A.D., Craddock, R.A., Moore, J.M., 2005b. An intense terminal epoch of widespread fluvial activity on early Mars: 2. Increased runoff and paleolake development. J. Geophys. Res. 110, E12S15. http://dx.doi.org/10.1029/2005JE002460.
Irwin III, R.P., Howard, A.D., Craddock, R.A., 2008. Fluvial valley networks on Mars. In: Rice, S.P., Roy, A.G., Rhoads, B.L. (Eds.), River Confluences, Tributaries and the Fluvial Network. John Wiley & Sons, Chichester, pp. 419–450.
Jackson, R.G.I., 1978. Preliminary evaluation of lithofacies models for meandering alluvial streams. In: Miall, A.D. (Ed.), Fluvial Sedimentology. Canadian Society of Petroleum Geologists, pp. 543–576.
Jackson, R.G.I., 1981. Sedimentology of muddy fine-grained channel deposits in meandering streams of the American Middle West. J. Sediment. Petrol. 51, 1169–1192.
Jones, B.M., Grosse, G., 2013. Extraction of lakes from an IfSAR DSM and a GIS-based analysis of drainage potential, Western Arctic Coastal Plain of northern Alaska. Report and Data for the Arctic Landscape Conservation Cooperative.
Jorgenson, T., Shur, Y., Osterkamp, T., Ping, C.-L., Kanevskij, M., 2011. Part 1: environment of the Beaufort Coastal Plain. In: Jorgenson, T. (Ed.), Coastal Region of Northern Alaska: Guidebook to Permafrost and Related Features. Alaska Division of Geological & Geophysical Surveys, Fairbanks, AK, pp. 1–39.
Kerber, L., Head, J.W., 2010. The age of the Medusae Fossae Formation: evidence of Hesperian emplacement from crater morphology, stratigraphy, and ancient lava contacts. Icarus 206, 669–684. http://dx.doi.org/10.1016/j.icarus.2009.1010.1001.
Kite, E.S., Williams, J.-P., Lucas, A., Aharonson, O., 2014. Low palaeopressure of the Martian atmosphere estimated from the size distribution of ancient craters. Nat. Geosci. http://dx.doi.org/10.1038/NGEO2137.
Kleinhans, M.G., 2005. Flow discharge and sediment transport models for estimating a minimum timescale of hydrological activity and channel and delta formation on Mars. J. Geophys. Res. 110, E12005. http://dx.doi.org/10.11029/12005JE002521.
Kleinhans, M.G., 2010. Sorting out river channel patterns. Prog. Phys. Geogr. 34, 287–326.
Knighton, A.D., Nanson, G.C., 1993. Anastomosis and the continuum of channel pattern. Earth Surf. Process. Landf. 18, 613–625.
Komar, P.D., 1979. Comparisons of the hydraulics of water flows on Martian outflow channels with flows of similar scale on Earth. Icarus 37, 156–181.
Komar, P.D., 1980a. Modes of sediment transport in channelized water flows with ramifications to the erosion of the Martian outflow channels. Icarus 42, 317–329.
Komar, P.D., 1980b. Channel meandering and braiding: are empirical equations based upon terrestrial rivers applicable to Mars? Reports of the Planetary Geology Program 1989, NASA Technical Memorandum 82385, pp. 361–363
Komatsu, G., Baker, V.R., 1997. Paleohydrology and flood geomorphology of Ares Vallis. J. Geophys. Res. Planets 102 (E2), 4151–4160.
Leopold, L.B., Wolman, M.G., 1957. River channel patterns: braided meandering, and straight. U.S. Geological Survey Professional Paper 282-B (85 pp.).
Leopold, L.B., Wolman, M.G., 1960. River meanders. Geol. Soc. Am. Bull. 71 (6), 769–793.
Lewellen, R.I., 1972. Studies of the Fluvial Environment — Arctic Coastal Plain Province Northern Alaska. Self-Published, Littleton, Colorado.
Long, D.G.F., 1978. Proterozoic stream deposits: some problems of recognition and interpretation of ancient sandy fluvial systems. In: Miall, A.D. (Ed.), Fluvial Sedimentology. Canadian Society of Petroleum Geologists, Calgary, Canada, pp. 313–341.
Louderback, L.A., Rhode, D.E., 2009. 15,000 years of vegetation change in the Bonneville basin: the Blue Lake pollen record. Quat. Sci. Rev. 28, 308–326.
Madsen, D.B., Rhode, D., Grayson, D.K., Broughton, J.M., Livingston, S.D., Hunt, J., Quade, J., Schmitt, D.N., Shaver III, M.W., 2001. Late Quaternary environmental change in the Bonneville Basin, Western USA. Palaeogeogr. Palaeoclimatol. Palaeoecol. 167 (3–4), 243–271.
Makaske, B., 2001. Anastomosing rivers: a review of their classification, origin and sedimentary products. Earth Sci. Rev. 53 (3–4), 149–196.
Malin, M.C., Edgett, K.S., 2003. Evidence for persistent flow and aqueous sedimentation on early Mars. Science 302, 1931–1934.
Malin, M.C., Bell III, J.F., Cantor, B.A., Caplinger, M.A., Calvin, W.M., Clancy, R.T., Edgett, K.S., Edwards, L., Haberle, R.M., James, P.B., Lee, S.W., Ravine, M.A., Thomas, P.C., Wolf, M.J., 2007. Context camera investigation on board the Mars Reconnaissance Orbiter. J. Geophys. Res. 112, E05S04. http://dx.doi.org/10.1029/2006JE002808.
Mandt, K.E., de Silva, S.L., Zimbelman, J.R., Crown, D.A., 2008. The origin of the Medusae Fossae Formation, Mars: insights from a synoptic approach. J. Geophys. Res. 113, E12011. http://dx.doi.org/10.11029/12008JE003076.
Mandt, K.E., de Silva, S.L., Zimbelman, J., Wyrick, D., 2009. Distinct erosional progressions in the Medusae Fossae Formation, Mars, indicate contrasting environmental conditions. Icarus 204 (2), 471–477.
Mangold, N., Ansan, V., Masson, P., Quantin, C., Neukum, G., 2008. Geomorphic study of fluvial landforms on the northern Valles Marineris plateau. J. Geophys. Res. 113, E08009. http://dx.doi.org/10.01029/02007JE002985.
Matsubara, Y., 2013. The Environment of Early Mars. (PhD Dissertation), University of Virginia, Charlottesville, Virginia (219 pp.).
Matsubara, Y., Howard, A.D., 2014. Modeling planform evolution of the mud-dominated meandering river: Quinn River, Nevada USA. Geomorphology http://dx.doi.org/10.1002/esp.3588.
McKenney, R., Jacobson, R.B., Wertheimer, R.C., 1995. Woody vegetation and channel morphogenesis in low-gradient, gravel-bed streams in the Ozark Plateau, Missouri and Arkansas. Geomorphology 13, 175–198.
Miall, A.D., 1996. The Geology of Fluvial Deposits: Sedimentary Facies, Basin Analysis, and Petroleum Geology. Springer-Verlag, Berlin.
Micheli, E.R., Kirchner, J.W., Larsen, E.W., 2004. Quantifying the effect of riparian forest versus agricultural vegetation on river meander migration rates, Central Sacramento River, California, USA. River Res. Appl. 20, 537–548. http://dx.doi.org/10.1012/rra.1756.
Millar, R.G., 2000. Influence of bank vegetation on alluvial channel patterns. Water Resour. J. 205, 59–75.
Minckley, T.A., Whitlock, C., Bartlein, P.J., 2007. Vegetation, fire, and climate history of the northwestern Great Basin during the last 14,000 years. Quat. Sci. Rev. 26, 2167–2184.
Moody, J.A., Pizzuto, J.E., Meade, R.H., 1999. Ontogeny of a flood plain. Geol. Soc. Am. Bull. 111 (2), 291–303.
Moore, J.M., Howard, A.D., Dietrich, W.E., Schenk, P.M., 2003. Martian layered fluvial deposits: implications for Noachian climate scenarios. Geophys. Res. Lett. 30, 2292. http://dx.doi.org/10.1029/2003GL019002.

Morgan, A.M., Howard, A.D., Hobley, D.E.J., Moore, J., M., Dietrich, W.E., Williams, R.M.E., Burr, D.M., Grant, J.A., Wilson, S.A., Matsubara, Y., 2014. Sedimentary and climatic environment of alluvial fans in the Martian Saheki crater and a comparison with terrestrial fans in the Atacama Desert. Icarus 229, 131–156.
Morrison, R.B., 1964. Lake Lahontan: geology of southern Carson Desert, Nevada. U.S. Geological Survey Professional Paper 401, pp. 1–156.
Murgatroyd, A.L., Ternan, J.L., 1983. Impact of afforestation on stream bank erosion and channel form. Earth Surf. Process. Landf. 8, 357–369.
Murray, A.B., Paola, C., 1994. A cellular-model of braided rivers. Nature 371 (6492), 54–57.
Nanson, G.C., 1980. Point bar and floodplain formation of the meandering Beatton River, northwestern British Columbia, Canada. Sedimentology 27, 3–29.
Nanson, G.C., Knighton, A.D., 1996. Anabranching rivers: their cause, character and classification. Earth Surf. Process. Landf. 21 (3), 217–239.
Newsom, H.E., Lanza, N.L., Ollila, A.M., Wiseman, S.M., Roush, T.L., Marzo, G.A., Tornabene, L.L., Okubo, C.H., Osterloo, M.M., Hamilton, V.E., Crumpler, L.S., 2010. Inverted channel deposits on the floor of Miyamoto crater, Mars. Icarus 205 (1), 64–72.
Odgaard, A.J., 1987. Streambank erosion along two rivers in Iowa. Water Resour. Res. 23, 1225–1236.
Ori, G.G., Cannarsa, F., Salese, F., Dell'Arciprete, I., Komatsu, G., 2013. Why braided streams are apparently absent but there are meander and low-sinuosity single-channel river systems on Mars. 44th Lunar and Planetary Science Conference, Abstract 2360.
Osman, A., Thorne, C., 1988. Riverbank stability analysis. I: theory. J. Hydraul. Eng. 114, 134–150.
Osterloo, M.M., Hamilton, V.E., Bandfield, J.L., Glotch, T.D., Baldridge, A.M., Christensen, P.R., Tornabene, L.L., Anderson, F.S., 2008. Chloride-bearing materials in the southern highlands of Mars. Science 319 (5870), 1651–1654.
Oviatt, C.G., Madsen, D.B., Schmitt, D.N., 2003. Late Pleistocene and early Holocene rivers and wetlands in the Bonneville basin of western North America. Quat. Res. 60, 200–210.
Page, K.J., Nanson, G.C., Frazier, P.S., 2003. Floodplain formation and sediment stratigraphy resulting from oblique accretion on the Murrumbidgee River, Australia. J. Sediment. Res. 73 (1), 5–14.
Pain, C., Clarke, J., Thomas, M., 2007. Inversion of relief on Mars. Icarus 190 (2), 478–491.
Parker, G., 1976. On the cause and characteristic scales of meandering and braiding in rivers. J. Fluid Mech. 76 (3), 457–480.
Parker, G., Wilcock, P.R., Paola, C., Dietrich, W.E., Pitlick, J., 2007. Physical basis for quasi-universal relations describing bankfull hydraulic geometry of single-thread gravel bed rivers. J. Geophys. Res. 112, F04005. http://dx.doi.org/10.1029/02006JF000549.
Parker, G., Shimizu, Y., Wilkerson, G.V., Eke, E.C., Abad, J.D., Lauer, J.W., Paola, C., Dietrich, W.E., Voller, V.R., 2011. A new framework for modeling the migration of meandering rivers. Earth Surf. Process. Landf. 36 (1), 70–86.
Pelletier, J.D., 2005. Formation of oriented thaw lakes by thaw slumping. J. Geophys. Res. F Earth Surf. 110 (Article Number F02018).
Pizzuto, J.E., Meckelnburg, T.S., 1989. Evaluation of a linear bank erosion equation. Water Resour. Res. 25 (5), 1005–1013.
Plug, L.J., West, J.J., 2009. Thaw lake expansion in a two-dimensional coupled model of heat transfer, thaw subsidence, and mass movement. J. Geophys. Res. 114 (F1), F01002. http://dx.doi.org/10.1029/02006JF000740.
Reheis, M.C., 1999. Extent of Pleistocene Lakes in the western Great Basin. U.S. Geological Survey, Miscellaneous Field Studies Map, MF-2323.
Rowland, J.C., Dietrich, W.E., Day, G., Parker, G., 2009. Formation and maintenance of single-thread tie channels entering floodplain lakes: observations from three diverse river systems. J. Geophys. Res. 114, F2013. http://dx.doi.org/10.1029/2008JF001073.
Ruff, S.W., Christensen, P.R., 2002. Bright and dark regions on Mars: particle size and mineralogical characteristics based on thermal emission spectrometer data. J. Geophys. Res. 107 (E12), 5127. http://dx.doi.org/10.1029/2001JE001580.
Schumm, S.A., 1960. The shape of alluvial channels in relation to sediment type. U.S. Geological Survey Professional Paper, P0352-B.
Schumm, S.A., 1963a. Sinuosity of alluvial rivers on the Great Plains. Geol. Soc. Am. Bull. 74 (9), 1089–1099.
Schumm, S.A., 1963b. A tentative classification of alluvial river channels. U.S. Geological Survey Circular 477 pp. 1–10.
Schumm, S.A., 1968a. Speculations concerning paleohydrologic controls of terrestrial sedimentation. Geol. Soc. Am. Bull. 79 (11), 1573–1588.
Schumm, S.A., 1968b. River adjustment to altered hydrologic regimen. Murrumbidgee River and paleochannels, Australia. U.S. Geological Survey Professional Paper P 0598. U.S. Geological Survey, Reston.
Schumm, S.A., Khan, H.R., 1971. Experimental study of channel patterns. Nature (London) 233 (5319), 407–409.
Schumm, S.A., Mosley, M.P., Weaver, W.E., 1987. Experimental Fluvial Geomorphology. John Wiley & Sons, New York.
Scott, K.M., 1978. Effects of permafrost on stream channel behavior in Arctic Alaska. U.S. Geological Survey Professional Paper 1068 pp. 1–19.
Scott, D.H., Tanaka, K.L., 1982. Ignimbrites of Anazonis Planitia region of Mars. J. Geophys. Res. 87 (B2), 1179–1190. http://dx.doi.org/10.1029/JB1187iB1102p01179.
Seminara, G., 2006. Meanders. J. Fluid Mech. 554, 271–297.
Seminara, G., Tubino, M., 1989. Alternate bars and meandering: free, forced and mixed interactions. In: Ikeda, S., Parker, G. (Eds.), River Meandering. American Geophysical Union, Washington, D.C., pp. 153–180.
Simon, A., Collison, A.J.C., 2002. Quantifying the mechanical and hydrologic effects of riparian vegetation on streambank stability. Earth Surf. Process. Landf. 27 (5), 527–546.
Simon, A., Curini, A., Darby, S.E., Langendoen, E.J., 1999. Streambank mechanics and the role of bank and near-bank processes in incised channels. In: Darby, S.E., Simon, A. (Eds.), Incised River Channels: Processes, Forms. Engineering and Management. Wiley, Chichester, pp. 123–152.
Smith, C.E., 1998. Modeling high sinuosity meanders in a small flume. Geomorphology 25, 19–30.
Tal, M., Gran, K., Murray, A.B., Paola, C., Hicks, D.M., 2004. Riparian vegetation as a primary control on channel characteristics in multi-thread rivers. In: Bennett, S.J., Simon, A. (Eds.), Riparian Vegetation and Fluvial Geomorphology. American Geophysical Union, Washington, D.C., pp. 43–58.
Tanaka, K.L., 1986. The stratigraphy of Mars. J. Geophys. Res. 91, 139.
Tchakerian, V.P., Lancaster, N., 2002. Late Quaternary arid/humid cycles in the Mojave Desert and western Great Basin of North America. Quat. Sci. Rev. 21, 799–810.
Thorne, C.R., 1990. Effects of vegetation on riverbank erosion and stability. In: Thornes, J.B. (Ed.), Vegetation and Erosion. John Wiley, Hoboken, N. J., pp. 125–143.
Thorne, C.R., Abt, S.R., 1993. Analysis of riverbank instability due to toe scour and lateral erosion. Earth Surf. Process. Landf. Tech. Softw. Bull. 18 (9), 835–843.
Thorne, C., Tovey, K., 1981. Stability of composite riverbanks. Earth Surf. Process. Landf. 6, 469–484.
Thorne, C.R., Alonso, C., Bettess, R., Borah, D., Darby, S., Diplas, P., Julien, P., Knight, D., Li, L.G., Pizzuto, J., Quick, M., Simon, A., Stevens, M., Wang, S., Watson, C., 1998a. River width adjustment. I: processes and mechanisms. J. Hydraul. Eng. ASCE 124 (9), 881–902.
Thorne, C.R., Alonso, C., Bettess, R., Borah, D., Darby, S., Diplas, P., Julien, P., Knight, D., Li, L.G., Pizzuto, J., Quick, M., Simon, A., Stevens, M., Wang, S., Watson, C., Kovacs, A., Mosselman, E., Schippa, L., Wiele, S., 1998b. River width adjustment. II: modeling. J. Hydraul. Eng. ASCE 124 (9), 903–917.
Tirsgaard, H., Oxnevad, I.E.I., 1998. Preservation of pre-vegetational mixed fluvio-aeolian deposits in a humid climatic setting: an example from the Middle Proterozoic Eriksfjord Formation. Southwest Greenl. Sediment. Geol. 120 (1–4), 295–317.
Trimble, S.W., 1997. Stream channel erosion and change resulting from riparian forests. Geology 25 (5), 467–469.
Trimble, S.W., 2004. The effect of riparian vegetation on stream channel stability and sediment budgets. In: Bennett, S.J., Simon, A. (Eds.), Riparian Vegetation and Fluvial Geomorphology. American Geophysical Union, Washington, D.C., pp. 153–169.
Van De Wiel, M.J., Darby, S.E., 2004. Numerical modeling of bed topography and bank erosion along tree-lined meandering rivers. In: Bennett, S.J., Simon, A. (Eds.), Riparian Vegetation and Fluvial Geomorphology. American Geophysical Union, Washington, D.C., pp. 267–282.
Van de Wiel, M.J., Darby, S., 2007. A new model to analyze the impact of woody riparian vegetation on the geotechnical stability of riverbanks. Earth Surf. Process. Landf. 32, 2185–2198.
van Dijk, W.M., van de Lageweg, W.I., Kleinhans, M.G., 2012. Experimental meandering river with chute cutoffs. J. Geophys. Res. 117 (F3). http://dx.doi.org/10.1029/2011JF002314.
Vandenberghe, J., 2001. A typology of Pleistocene cold-based rivers. Quat. Int. 79, 111–121.
Vandenberghe, J., 2002. The relation between climate and river processes, landforms and deposits. Quat. Int. 91 (1), 17–23.
Walker, H.J., Arnborg, L., 1966. Permafrost and ice-wedge effects on riverbank erosion. Permafrost: International Conference. National Research Council Publication 1287, Lafayette, Indiana, pp. 164–171.
Walker, H.J., Hudson, P.F., 2003. Hydrologic and geomorphic processes in the Colville River delta, Alaska. Geomorphology 56 (3–4), 291–303.
Walker, H.J., Jorgenson, T., 2011. Part 4: tour of the Colville river delta. In: Jorgenson, T. (Ed.), Coastal Region of Northern Alaska: Guidebook to Permafrost and Related Features. Alaska Division of Geological & Geophysical Surveys, Fairbanks, AK, pp. 85–135.
Walker, H.J., Arnborg, L., Peippo, J., 1987. Riverbank erosion in the Colville Delta, Alaska. Geogr. Ann. Ser A Phys. Geog. 69 (1), 61–70.
Ward, A.W., 1979. Yardangs on Mars — evidence of recent wind erosion. J. Geophys. Res. 84, 8147–8166.
Werner, S.C., 2006. Major aspects of the chronostratigraphy and geologic evolutionary history of Mars. (Freie Universität, available from www.diss.fu-berlin.de/2006/33/indexe.ht).
West, J.J., Plug, L.J., 2008. Time-dependent morphology of thaw lakes and taliks in deep and shallow ground ice. J. Geophys. Res. 113 (F1), F01009. http://dx.doi.org/10.1029/02006JF00696.
Wilkerson, G.V., Parker, G., 2011. Physical basis for quasi-universal relationships describing bankful hydraulic geometry of sand-bed rivers. J. Hydraul. Eng. 137, 739–753.
Williams, J.R., 1983. Engineering-geologic maps of northern Alaska, Mead River Quadrangle. U.S. Geological Survey Open File Report 83-294.
Williams, G.P., 1986. River meanders and channel size. J. Hydrol. 88 (1–2), 147–164.
Williams, G.P., 1988. Paleofluvial estimates from dimensions of former channels and meanders. In: Baker, V.R., Kochel, R.C., Patton, P.C. (Eds.), Flood Geomorphology. John Wiley & Sons, New York, pp. 321–334.
Williams, R.M.E., 2007. Global spatial distribution of raised curvilinear features on Mars. Lunar and Planetary Sci. Conf. XXXVIII, Abstract 1821.
Williams, R.M.E., Edgett, K.S., 2005. Valleys in the Martian rock record. 36th Annual Lunar and Planetary Science Conference (pp. Abstract 1099).
Williams, J.R., Yeend, W.E., Carter, L.D., Hamilton, T.D., 1977. Preliminary surficial deposits map, National Petroleum Reserve, Alaska. U.S. Geological Survey Open File Report 77-868.
Williams, J.R., Carter, L.D., Yeend, W.E., 1978. Coastal plain deposits of NPRA. In: Johnson, K.M. (Ed.), The United States Geological Survey in Alaska: Accomplishments During 1997. USGS Circular 772-B, pp. B20–B22.
Williams, R.M.E., Irwin, R.P., Zimbelman, J.R., 2009. Evaluation of paleohydrologic models for terrestrial inverted channels: implications for application to Martian sinuous ridges. Geomorphology 107 (3–4), 300–315.

Williams, R.M.E., Irwin, R.P.I., Burr, D.M., Harrison, T., McClelland, P., 2013. Variability in Martian sinuous ridge form: case study of Aeolis Serpens in the Aeolis Dorsa, Mars, and insight from the Mirackina paleoriver, South Australia. Icarus 225, 308–324.

Wilson, L., Ghatan, G.J., Head, I.J.W., Mitchell, K.L., 2004. Mars outflow channels: a reappraisal of the estimation of water flow velocities from water depths, regional slopes, and channel floor properties. J. Geophys. Res. E Planets 109 (9), E09003 (09001-09010).

Wolman, M.G., Leopold, L.B., 1957. River flood plains: some observations on their formation. U.S. Geological Survey Professional Paper P0282-C, pp. 87–109.

Wood, A.L., Simon, A., Downs, P.W., Thorne, C.R., 2001. Bank-toe processes in incised channels: the role of apparent cohesion in the entrainment of failed bank materials. Hydrol. Process. 15 (1), 39–61.

Zimbelman, J.R., Griffin, L.J., 2010. HiRISE images of yardangs and sinuous ridges in the lower member of the Medusae Fossae Formation, Mars. Icarus 205, 198–210.

Zimbelman, J.R., Scheidt, S.P., 2012. Hesperian age for western Medusae Fossae Formation, Mars. Science 336, 1683.

Zimmerman, R.C., Gootlett, J.C., Comer, G.H., 1967. The influence of vegetation on channel form of small streams. Symposium on river morphology. Int. Assoc. Sci. Hydrol. 75, 255–275.